

UCLA

UCLA Electronic Theses and Dissertations

Title

ACTIVATION MECHANISM AND NOVEL THERAPEUTIC AGENT OF A MEMBRANE RECEPTOR INVOLVED IN PATHOGENIC ANGIOGENESIS

Permalink

<https://escholarship.org/uc/item/62n4m0jh>

Author

Au, Adrian Chichuen

Publication Date

2020

Peer reviewed|Thesis/dissertation

UNIVERSITY OF CALIFORNIA

Los Angeles

**ACTIVATION MECHANISM AND NOVEL THERAPEUTIC AGENT OF A
MEMBRANE RECEPTOR INVOLVED IN PATHOGENIC ANGIOGENESIS**

A dissertation submitted in partial satisfaction of the requirements for the degree

Doctor of Philosophy in Molecular, Cellular, and Integrative Physiology

by

Adrian Au

2020

© Copyright by

Adrian Au

2020

ABSTRACT OF THE DISSERTATION

**Activation Mechanism and Novel Therapeutic Agent of a
Membrane Receptor Involved in Pathogenic Angiogenesis**

by

Adrian Au

Doctor of Philosophy in Molecular, Cellular, and Integrative Physiology

University of California, Los Angeles, 2020

Professor Hui Sun, Chair

Pigment epithelial derived factor (PEDF) is a natural ligand with a wide range of therapeutic functions. It was first characterized as a neurotrophic factor secreted by the retinal pigment epithelium (RPE) but later found to be a potent anti-angiogenic factor that acts independent of vascular endothelial growth factor (VEGF). As a result, PEDF garnered significant attention from industry and academia but progress in leveraging PEDF's ability was hampered by the lack of insight in its signaling mechanism. After 20 years from its initial identification, the cell surface receptor responsible for PEDF's anti-angiogenic effect was found to be tumor endothelial marker 7 (TEM7) or plexin-domain containing 1 (PLXDC1). This receptor was found to be highly

expressed in the endothelium of a wide range of solid tumors (e.g. pancreatic and colon cancer) and vision disease (e.g. diabetic retinopathy and age-related macular degeneration).

To transform the power of PEDF into an anti-angiogenic therapy that can treat human disease, we focused on two main goals. The first was to elucidate how PLXDC1 receptor activation causes endothelial cell death. The second is to develop antibodies that can diagnose endogenous PLXDC1 expression and that can kill pathogenic blood vessels through PLXDC1 receptor activation. Receptors are ideal therapeutic targets due to their accessibility and ability to regulate cell outcomes. Although no receptor activating antibody is currently used clinically, antibodies are an ideal drug as they are highly specific with minimal off-target toxicity.

With the use of a small molecule PLXDC1 agonist, we found that the mechanism of PLXDC1-mediated endothelial cell death is consistent with anoikis, a detachment induced cell death pathway. We observed that a small molecule PLXDC1 agonist inhibited cell adhesion, which caused cell detachment, re-localization of beta-catenin, de-phosphorylation of focal adhesion kinase, and ultimately cell death. Independently, integrin beta-1 (ITGB1), a transmembrane protein involved in attaching endothelial cells to the extracellular matrix, was identified as a binding partner to PLXDC1 by unbiased affinity purification/mass spectrometry. We also discovered that ITGB1 not only bound to PLXDC1, but at higher levels in the activated form of PLXDC1. This was functionally confirmed by enhanced PEDF mediated receptor activation with co-expression of ITGB1 and inhibition of PEDF induced endothelial cell death with knockdown of ITGB1.

Separately, we produced monoclonal and fragment antigen binding (Fab) antibodies that detect and kill pathogenic blood vessels through hybridoma and phage display strategies. Amongst the 96 mouse monoclonal antibodies, we identified three antibodies that reliably detected PLXDC1 in a wide range of human cancers. We then screened over 200 billion human Fabs for antibodies that could preferentially bind the activated receptor. Amongst those, we developed 30 antibodies that can inhibited cell adhesion, induced cell detachment, and caused endothelial cell death *in vitro* and *ex vivo*. Lastly, we demonstrate that a few of those antibodies showed ability to inhibit laser induced choroidal neovascularization progression *in vivo* with intravitreal injections.

In summary, we have identified the mechanism of PLXDC1 mediated endothelial cell death and developed diagnostic and therapeutic antibodies targeting PLXDC1. Combined this provides further insight into how we can translate PEDF's natural anti-angiogenic potential into a therapy to treat human cancer and vision disease.

The dissertation of Adrian Au is approved.

Dean Bok

Gabriel Travis

Roxana Radu

Hui Sun, Committee Chair

University of California, Los Angeles

2020

DEDICATION

I dedicate my thesis to my wife Kelley and my future son.

In science, failure comes easy and often; but with you, it is easily forgotten.

Rain or shine, you are the constants in my life.

I love you, always and forevermore.

TABLE OF CONTENTS

Abstract of dissertation	ii
Table of Contents	vii
List of Tables	xi
List of Figures	xii
Acknowledgements	xiv
Biographic Sketch	xv
Chapter 1: Introduction	1
1.1 Anti-angiogenesis and pigment epithelial derived factor (PEDF)	1
1.1.1 Angiogenesis and blood vessel-related human disease	1
1.1.2 Current anti-angiogenesis therapies, their success and limitations	1
1.1.3 Retinal pigment epithelial derived factor (PEDF) – a potent anti-angiogenic factor	3
1.2 Identification of PEDF receptors: PLXDC1 and PLXDC2	4
1.3 PLXDC1 (TEM7), a specific target on pathogenic blood vessels	5
Chapter 2: Mechanism of signaling transduction of PLXDC1	9
2.1 Introduction to signal transduction cascades	9
2.2 Comparison of unbiased approaches to identifying down-stream signaling proteins	9
2.3 Mechanism of PEDF-PLXDC1 receptor interaction	11
2.4 Detachment-induced cell death: anoikis	11
2.5 Materials and Methods	12
2.5.1 Cell culture and cell lines	12
2.5.2 Gene engineering and constructs	13
2.5.3 Tryptophan intrinsic fluorescence	14

2.5.4 Genome-wide CRISPR Knockout (GeCKO).....	14
2.5.5 Functional cell assays	16
2.5.5.1 Cell receptor activation assay	16
2.5.5.2 Cell adhesion assay	16
2.5.5.3 Endothelial cell death assay	17
2.5.6 siRNA-mediated knockdown.....	17
2.5.7 Western blot analysis	18
2.5.8 Co-purification: co-immunoprecipitation and western blot.....	19
2.6 Results.....	19
2.6.1.1 Small molecule PLXDC1 agonist binds to PLXDC1 and causes conformational change	
2.6.1.2 Small molecule PLXDC1 agonist causes anoikis, detachment induced cell death	20
2.6.1.3 Genome-wide knock-out screening identifies genes involved in PLXDC1 mediated cell death	20
2.6.1.4 PLXDC1-mediated cell death depends on integrin beta 1	21
2.7 Discussion.....	22
Chapter 3: Development of a therapeutic antibody targeting PLXDC1	40
3.1 Introduction of modern therapeutic antibodies and potential significance.....	40
3.2 Current strategies for monoclonal antibody development.....	40
3.3 Overview of screening strategy	42
3.4 Materials and Methods.....	43
3.4.1 Large scale PLXDC1 protein production and purification	43
3.4.2 Mouse monoclonal antibody production.....	44

3.4.3 Large scale human library antibody screening.....	44
3.4.4 Antibody binding assays: ELISA, western blot, and immunohistochemistry.....	45
3.4.5 <i>In vitro</i> assays of receptor activation.....	47
3.4.5.1 Cell receptor activation assay	47
3.4.5.2 Cell adhesion assay.....	47
3.4.5.3 Endothelial cell death assay.....	48
3.4.6 <i>Ex vivo</i> 3D endothelial cell culture.....	48
3.4.6.1 Lentivirus transfection of 3D endothelial cell culture.....	48
3.4.7 <i>In vivo</i> endothelial cell culture	49
3.4.7.1 Humanized transgenic mouse model.....	49
3.4.7.2 Laser induced choroidal neovascularization and intravitreal injections.....	50
3.5 Results.....	51
3.5.1 Novel mouse monoclonal antibodies bind and identify recombinant and endogenous PLXDC1	51
3.5.2 Novel mouse monoclonal antibodies activate PLXDC1 and cause endothelial cell death	52
3.5.3 Human Fab library screen yielded highly enriched antibodies that preferentially bind the activate PLXDC1	53
3.5.4 Human Fabs inhibit endothelial cell adhesion and cause secondary endothelial cell death	53
3.5.5 Human Fabs cause endothelial cell death in <i>ex vivo</i> endothelial cell culture.....	54
3.5.6 Human Fabs cause partial inhibition of CNV in a laser-induced retinopathy model.....	54
3.6 Discussion.....	55

References70

LIST OF TABLES

Table 1-1 Disadvantages of anti-VEGF therapy

Table 2-1 List of reagents and equipment

Table 3-1 List of cell lines, reagents, and equipment

LIST OF FIGURES

Figure 2-1 Proposed mechanism of PLXDC1 activation

Figure 2-2 Inducible PLXDC1 constructs

Figure 2-3 Genome-wide CRISPR-Cas9 knockout screening approach

Figure 2-4 Small molecule PLXDC1 agonist binds to and causes PLXDC1 conformational change

Figure 2-5 Small molecule PLXDC1 agonist induces anoikis in endothelial cells

Figure 2-6 Beta-catenin localization with small molecule PLXDC1 agonist treatment

Figure 2-7 Phosphorylation of focal adhesion kinase in small molecule PLXDC1 agonist treatment

Figure 2-8 Genome wide CRISPR-Cas9 Knockout (GeCKO) provides selective advantage in small molecule PLXDC1 agonist treatment

Figure 2-9 Expression of activated PLXDC1 receptor causes cell death

Figure 2-10 Genome wide CRISPR-Cas9 Knockout (GeCKO) screening

Figure 2-11 siRNA knockdown of ITGB1 inhibits small molecule PLXDC1 agonist cell death

Figure 2-12 PLXDC1 specific receptor activation is enhanced with ITGB1 co-transfection

Figure 2-13 Co-immunoprecipitation of Rim-tagged full length and deletional constructs of PLXDC1 with ITGB1

Figure 3-1 Genomic engineering strategy for knock-in PLXDC1 transgenic mouse

Figure 3-2 Purification of PLXDC1

Figure 3-3 Example of ELISA from hybridoma mouse monoclonal antibody

Figure 3-4 Monoclonal mouse antibodies recognize recombinant PLXDC1

Figure 3-5 Live cell staining of HEK293 ectopically expressing PLXDC1

Figure 3-6 Immunohistochemistry with anti-human PLXDC1 mouse monoclonal antibody

Figure 3-7 Mouse monoclonal antibody causes endothelial cell death in human *ex vivo* 3D endothelial cell culture

Figure 3-8 Mouse monoclonal antibody causes endothelial cell death in mouse *ex vivo* 3D endothelial cell culture

Figure 3-9 SDS-Page show presence of purified Fabs

Figure 3-10 ELISA of Fab binding affinity between activated and non-activated receptor

Figure 3-11 Human Fabs cause endothelial cell death *in vitro*

Figure 3-12 Human Fabs cause endothelial cell death in *ex vivo* 3D endothelial cell culture

Figure 3-13 Human Fabs cause inhibition of *in vivo* laser-induced choroidal neovascularization

ACKNOWLEDGEMENTS

My deepest gratitude and appreciation go to the Sun lab, who have given me an environment to think big and grow. To Dr. Sun: there are few scientists daring enough to dream of making this world a better place. You have shown me that it's possible to not only dream but also to make it a reality. I am forever indebted to you for allowing me to be a part of history. To Guo: I appreciate all the help and insight you have provided me throughout our time together. Stay motivated and keep growing, you have so much potential to share with others. To Crystal and Emily: it was a privilege to teach and learn from you guys. Remember to pass on the knowledge! I look forward to what great things you will do in the future.

Thank you to my thesis committee Drs. Bok, Travis, and Radu for giving me the opportunity to present my work and your thoughtful suggestions.

To my parents, grandparents, siblings, new family (Isa and the Lowes), and close friends, you guys are the reason I even have the opportunity to write this thesis. You provide the quiet, consistent, and unequivocal support that keeps me balanced. Thank you.

Lastly, I would like to thank the patients that have provided their tissue to this project. Although we may have never met, you have given us the opportunity to hopefully treat those in the future.

BIOGRAPHIC SKETCH

EDUCATION

Olive-View Medical Center, University of California, Los Angeles, Sylmar, CA

Intern, 07/16 – 07/17

Case Western Reserve University School of Medicine, Cleveland, OH

Doctor of Medicine, 07/11 – 05/16

University of Southern California, Los Angeles, CA

Bachelor of Arts, *magna cum laude*, Phi Beta Kappa, Neuroscience, 09/07 - 05/11

HONORS / SOCIETY

Rose Hill Foundation Research Fellow (2010)

HHMI-FFB Medical Research Fellow (2014-2015)

PUBLICATIONS

1. Gerka-Stuyt J*, **Au A***, Peachey NS, Alagramam KN. (2013). Transient receptor potential melastatin 1: a hair cell transduction channel candidate. *PLoS ONE*, 8(10) doi:10.1371/journal.pone.0077213.
2. **Au A**, Stuyt JG, Chen D, Alagramam K. (2013). Ups and Downs of Viagra: Revisiting Ototoxicity in the Mouse Model. *PLoS ONE*, 8(11) doi:10.1371/journal.pone.0079226.
3. **Au A**, Parikh VS, Modi YS, Ehlers JP, Schachat AP, Singh RP (2015). Hydroxychloroquine Screening Practice Patterns within a Large Multispecialty Ophthalmic Practice. *American Journal of Ophthalmology*. doi: 10.1016/j.ajo.2015.06.009.
4. Parikh VS, Modi YS, **Au A**, Ehlers JP, Srivastava SK, Schachat AP, Singh RP (2016) Non-Leaking Cystoid Macular Edema as a Presentation of Hydroxychloroquine Retinal Toxicity. *Ophthalmology*. doi: 10.1016/j.ophtha.2015.09.011
5. **Au A** and Singh RP (2016). Multimodal approach to diabetic macular edema. *Journal of Diabetic Complications*. doi: 10.1016/j.jdiacom.2015.11.008
6. Lobo G, **Au A***, Kiser PD, Hagstrom SA (2016) Involvement of Endoplasmic Reticulum Stress in TULP1 Induced Retinal Degeneration. *PLoS ONE* 11(3). doi: 10.1371/journal.pone.0151806
7. Modi YS*, **Au A***, Parikh VS, Ehlers JP, Schachat AP, Singh RP (2016) Volumetric Single-Layer Inner Retinal Analysis in Patients with Hydroxychloroquine. *Retina* 36(10). doi: 10.1097/IAE.0000000000001036
8. Parikh VS, **Au A**, Modi YS, Schachat AP, Rodstrom T, Singh RP. Impact of an Electronic Decision Support Tool on Hydroxychloroquine Screening. (2016) *Ophthalmology* 123(11). doi: 10.1016/j.ophtha.2016.06.056
9. **Au A**, Parikh VS, Singh RP, Ehlers JP, Yuan A, Rachitskaya AV, Sears JE, Srivastava SK, Kaiser PK, Schachat AP, Martin DF, Modi Y (2017) Comparison of anti-VEGF

- therapies on fibrovascular pigment epithelial detachments in age-related macular degeneration. *Br J Ophthalmol* 101(7): 970-975. doi: 10.1136/bjophthalmol-2016-309434
10. Pichi F, Fragiotta S, Freund KB, **Au A**... Sarraf D (2018) Cilioretinal artery hypoperfusion and its association with paracentral acute middle maculopathy. *Br J Ophthalmol*. doi: 10.1136/bjophthalmol-2018-312774
 11. **Au A**, Hou K, Baumal CR, Sarraf D (2018) Radial Hemorrhage in Henle Layer in Macular Telangiectasia Type 2. *JAMA Ophthalmol* 136(10)11825-1185. doi 10.1001/jamaophthalmol.2018.2979.
 12. **Au A**, Sarraf D (2018) Vascular anatomy and its relationship to pathology in retinoschisis. *Eye (Lond)* doi: 10.1038/s41433-018-0298-6
 13. Govetto A, Hubschman JP, Sarraf D...**Au A**, et al (2020). The role of Muller cells in tractional macular disorders: an optical coherence tomography study and physical model of mechanical force transmission. *Br J Ophthalmol*. doi: 10.1136/bjophthalmol-2019-314245
 14. **Au A**, Hou K, Davila JP, et al. Volumetric Analysis of Vascularized Serous Pigment Epithelial Detachment Progression in Neovascular Age-Related Macular Degeneration Using Optical Coherence Tomography Angiography (2019). *Invest Ophthalmol Vis Sci*. doi: 10.1167/iovs.18-26478.
 15. Iovino C, **Au A**, Hilely A, et al. Evaluation of Choroid in Eyes With Retinitis Pigmentosa and Cystoid Macular Edema (2019). *Invest Ophthalmol Vis Sci*. doi: 10.1167/iovs.19-27300.
 16. Govetto A, Sarraf, D, Hubschman JP...**Au A**, et al. Distinctive Mechanisms and Patterns of Exudative Versus Tractional Intraretinal Cystoid Spaces as Seen With Multimodal Imaging (2020). *Am J Ophthalmol*. doi: 10.1016/j.ajo.2019.12.010
 17. Lenis TL, **Au A**, Hou K, Govetto A, Sarraf D (2020). Alterations of the foveal central bouquet associated with cystoid macular edema. *Can J Ophthalmol*. doi: 10.1016/j.jcjo.2020.01.013
 18. Iovino C, **Au A**, Chhablani J, et al. (2020) Choroidal anatomical alterations following photodynamic therapy for chronic central serous chorioretinopathy: a multicenter study. *Am J Ophthalmol*. doi: 10.1016/j.ajo.2020.04.022
 19. **Au A**, Hilely A, Scharf J, et al. Relationship between Nerve Fiber Layer Hemorrhages and Outcomes in Central Retinal Vein Occlusion (2020). *Invest Ophthalmol Vis Sci*. doi: 10.1167/iovs.61.5.54.

PATENTS

1. KILLING TUMORS BY TARGETING PLXDC1/PLXDC2 ON TUMOR BLOOD VESSELS (2019-996-1-US)
2. COMPOSITIONS AND METHODS FOR DETECTING PLXDC1 AND PLXDC2 IN HUMAN ISSUES (2019-733-1-US)
3. EX VIVO TUMOR ANGIOGENESIS MODEL (2019-615-1-US)
4. COMPOUNDS AND METHODS FOR TARGETING PATHOGENIC BLOOD VESSELS (2019-614-1-US)

CHAPTER 1: INTRODUCTION

1.1 Anti-angiogenesis and pigment epithelial derived factor (PEDF)

1.1.1 Angiogenesis and blood vessel-related human disease

Blood is the essential life force that transports nutrients and metabolic waste to and from cells. In normal physiology, it is conveyed in a well-structured and developed network of vessels ranging from arteries, veins, and capillaries. The primary exchange of nutrients occurs within capillaries, where metabolically active tissues can readily access oxygen and nutrients. Capillary walls are lined with endothelium, a cell monolayer that plays a primary role in regulating the rate and flow of blood through capillaries. In pathologic states where metabolic demand outweighs supply, endothelial cells proliferate and grow from existing vasculature. This process is called angiogenesis.

Angiogenesis was first recognized in 1794 by a Scottish anatomist and surgeon John Hunter but was later proposed as a therapeutic target in 1971 by Judah Folkman.^{1,2} Folkman hypothesized that as tumor growth was dependent on new blood vessels, cancer could be treated by targeting angiogenesis. Since then evidence has supported the presence of pathologic angiogenesis in a variety of disease states, such as cancer, age-related macular degeneration (AMD), diabetic retinopathy, rheumatoid arthritis, and psoriasis.³⁻⁸ These findings spurred the development of therapeutic agents against the development of pathologic angiogenesis. However, a therapeutic agent that can preferentially target pathologic blood vessels still does not exist clinically. The current therapy only achieves partial inhibition.

1.1.2 Current anti-angiogenesis therapies, their success and limitations

The most notable therapeutic targeting anti-angiogenesis is anti-VEGF.⁹ Since the first recombinant monoclonal antibody neutralizing VEGF in 1994 (bevacizumab), anti-VEGF has revolutionized the management of angiogenetic dependent diseases of the eye, such as neovascular AMD and diabetic retinopathy.¹⁰ Multiple clinical trials have confirmed significant visual acuity improvements from anti-VEGF's ability to reduce vascular leakage causing macular edema.¹⁰ Despite this, many patients require recurrent anti-VEGF injections (almost monthly injections) with neovascularization progressing despite treatment. In some cases, patients are recalcitrant to anti-VEGF altogether.^{11,12} This has a significant burden both on the patient and health care system.

VEGF depletion may be detrimental for normal physiology. VEGF is necessary in the normal maintenance of the choriocapillaris and cones as in RPE-specific Cre-mediated deletion of *Vegfa*, choriocapillaris and cone degeneration rapidly occurs.^{13,14} Separately, some patients treated with a high affinity single-chain fragment against VEGF-A (brolucizumab) developed occlusive vasculitis. Some studies have suggested that this may be a consequence of on-target toxicity, where brolucizumab's higher affinity towards VEGF-A and higher concentration deplete the necessary maintenance VEGF within the eye.^{15,16}

Systemic administration of anti-VEGF, specifically for cancer, has been less successful with significant on-target side effects. Despite growth inhibition in colon cancer mouse models, bevacizumab showed no efficacy as monotherapy.^{17,18} When bevacizumab was used as an adjuvant chemotherapy, overall survival, progression-free survival, and response rate improved in metastatic colorectal cancer, metastatic renal cell carcinoma, and recurrent metastatic cervical cancer.¹⁹ This garnered its FDA approval.²⁰ Yet, there was still no effect in breast or pancreatic

cancer.¹⁹ As monotherapy, bevacizumab showed modest effects in 20-25% of patients with glioblastoma multiforme.^{21,22} Despite these positive effects, routine clinical use has been limited by its systemic side effects, such as arterial thromboembolic events (e.g. strokes, myocardial infarctions), gastrointestinal perforations, and severe or fatal hemorrhages.^{19,20} Therefore, anti-angiogenesis as a therapeutic approach has not been fully realized. This allows for the identification and evaluation of more specific anti-angiogenic targets.

1.1.3 Retinal pigment epithelial derived factor (PEDF) – a potent anti-angiogenic factor

Despite the benefits of targeted anti-VEGF, alternative anti-angiogenic pathways that are independent of VEGF need to be explored. One such anti-angiogenic ligand is retinal pigment epithelial derived factor (PEDF), a 418 amino acid protein that belongs to the non-inhibitory serpin protease inhibitor (serpin) family.²³ First isolated in 1989 by Tombran-Tink and Johnson in conditioned medium from fetal human retinal pigment epithelial (RPE) cell cultures, PEDF was first considered a potent neuronal differentiating ligand.²⁴⁻²⁶ It was surprisingly later determined to be the most potent anti-angiogenic factor.²⁷

One of the most important functions of PEDF is its ability to inhibit blood vessel growth. PEDF was first reported to prevent ocular vascularization in a groundbreaking study by Dawson et al. in 1999.²⁷ In this unbiased search for novel antiangiogenic factors, PEDF was identified as a potent anti-angiogenic factor by purification of fractionated media conditioned by retinoblastoma cells. Purified PEDF inhibited endothelial cell migration in the presence of vascular endothelium growth factor and impeded corneal neovascularization in the presence of basic fibroblast growth factor

(bFGF). In fact, PEDF counteracted VEGF and bFGF neovascularization at 2 nM and 8 nM respectively.²⁷

Other *in vitro* and *in vivo* studies confirmed PEDF's ability to regulate endothelial cell growth. PEDF counteracts proangiogenic factors and suppresses microvascular endothelial cell proliferation, migration and tube formation.²⁸⁻³⁰ In PEDF knockout mice, blood vessel density dramatically increases in retina, prostate, kidney and pancreas compared to wild-type mice.³¹ In disease models, PEDF treatment results in a reduction of microvascular density in a variety of malignancy including pancreatic adenocarcinoma, melanoma, neuroblastoma, prostate cancer, cervical cancer, and lung cancer.^{32,33} Combined, the evidence validates PEDF as a potent anti-angiogenic factor that is independent of VEGF. The identification of PEDF's receptor would allow the development of novel therapeutics that activate this effective pathway.

1.2 Identification of PEDF receptors: PLXDC1 and PLXDC2

In 2000, a seminal study by St. Croix et al. compared gene expression patterns on endothelial cells from normal and malignant colorectal cancer.³⁴ Using serial analysis of gene expression (SAGE), they validated the expression of nine tumor endothelial markers (TEM1 through TEM9). This diverse set of cell surface proteins, categorized phenotypically by their presence in tumor endothelial cells, are predicted to have very different functions. For example, TEM7 is a single transmembrane protein that contains a plexin-like domain with a short cytoplasmic tail, while TEM5 is a seven-pass transmembrane protein that shares homology with the secretin family of G-protein coupled receptors (GPCR).³⁵ Little is known about each of these TEM proteins but TEM7 is present in a wide-variety of angiogenic dependent diseases. TEM7 has been identified

specifically in pathogenic blood vessels associated with solid tumors such as colorectal³⁶, ovarian³⁷, glioblastoma³⁸, gastric³⁹, and renal⁴⁰ cancer. In addition, qualitative PCR of fibrovascular membranes in diabetic retinopathy patients confirms presence of TEM7 expression.⁴¹ Separately, our lab has found TEM7 in ischemia-induced retinopathy (or retinopathy of prematurity) and choroidal neovascularization. This suggest that TEM7 is a potential cell surface receptor present and specific to pathogenic blood vessels.

Although the function of TEM7 remains unknown, Cheng et al. found that TEM7 was the receptor for the most potent anti-angiogenic factor: PEDF.⁴² They identified the receptor by screening a library of orphan receptors that bound PEDF. They found that the previously phenotypically named TEM7 was in fact PLXDC1. This was confirmed by cell surface binding of PEDF to PLXDC1 and its homolog PLXDC2. Furthermore, they functionally confirmed through loss and gain of function assays that receptor signaling was activated by addition of PEDF in macrophages, neurons, and mouse endothelial cells.⁴²

1.3 PLXDC1 (TEM7), a specific target on pathogenic blood vessels

In 2000, a seminal study by St. Croix et al. compared gene expression patterns on endothelial cells from normal and malignant colorectal cancer.³⁴ Using serial analysis of gene expression (SAGE), they validated the expression of nine tumor endothelial markers (TEM1 through TEM9). This diverse set of cell surface proteins, categorized phenotypically by their presence in tumor endothelial cells, are predicted to have very different functions. For example, TEM7 (PLXDC1) is a single transmembrane protein with a short cytoplasmic tail contains a plexin-like domain, while TEM5 is a seven-pass transmembrane protein that shares homology with the secretin family of g-

protein coupled receptors (GPCR).³⁵ Little is known about each of these TEM proteins but TEM7 (PLXDC1) is known to be present in a wide-variety of angiogenic dependent diseases. TEM7 (PLXDC1) has been identified specifically in pathogenic blood vessels associated with solid tumors such as colorectal³⁶, ovarian³⁷, glioblastoma³⁸, gastric³⁹, and renal⁴⁰ cancer. In addition, qualitative PCR of fibrovascular membranes in diabetic retinopathy patients confirms presence of TEM7 (PLXDC1) expression.⁴¹ Separately, our lab has found TEM7 (PLXDC1) in ischemia-induced retinopathy (or retinopathy of prematurity) and choroidal neovascularization (Table 1-2). This suggest that TEM7 (PLXDC1) is a potential cell surface receptor present and specific to pathogenic blood vessels.

Targeting PLXDC1 is a novel, independent anti-angiogenic strategy that may have major implications in treating human disease. As PLXDC1 is naturally highly expressed in angiogenic diseases, developing first-in-class small molecule or antibody therapies would have significant impact in cancer and vision disease. In addition, PLXDC1-targeted therapy can target and kill pathogenic blood vessels, reducing the incomplete efficacy and on-target toxicity seen in anti-VEGF.

In conclusion, anti-angiogenesis as a therapeutic strategy is important in mitigating a wide-variety of human disease. Despite the significant improvement in morbidity and mortality with therapies targeting VEGF, its therapeutic limit may be reached as on-target toxicity may outweigh on-target effects at higher concentrations. Therefore, identification of novel therapeutic approaches for anti-angiogenesis is necessary. Pigment epithelial derived factor, a naturally expressed protein from RPE cells, was found to be a potent anti-angiogenesis agent. Interestingly, the receptor of PEDF,

identified as PLXDC1 or TEM7, is highly specifically expressed in pathogenic blood vessels. Now with the identification of its receptor, the objective of this thesis is to understand the PLXDC1 signaling transduction cascade and to develop a novel antibody that can leverage this pathway and cause endothelial cell death.

Table 1-1 Disadvantages of anti-VEGF therapy

Route of Administration	Disadvantages of Anti-VEGF Therapy
Systemic	<ul style="list-style-type: none">• VEGF is essential for normal blood vessels (no specificity for pathogenic blood vessels)• Anti-VEGF treatment has severe systemic toxicity• VEGF is only one of many angiogenic factors• Inhibits but does not effectively kill pathogenic blood vessels (allowing resistance to develop)• Limited effect in cancer treatment
Local	<ul style="list-style-type: none">• Non-responders (cannot inhibit in 1/3 of patients)• Even for responders, anti-VEGF cannot effectively kill pathogenic blood vessels• Limited to inhibition / reduction of leakage• Unknown effects of long-term suppression• Burden on patients and health care system as the choroidal neovascularization persists

CHAPTER 2: MECHANISM OF SIGNAL TRANSDUCTION OF PLXDC1

2.1. Introduction to signal transduction cascades

One important function of cell surface receptors is to regulate a cell's response to extracellular molecules. Cheng et al. have shown that PLXDC1 is a bona-fide cell surface receptor as it fulfills key features of membrane receptors: 1) localized to the plasma membrane, 2) confers cell surface binding to an extracellular ligand, and 3) mediates cell signal transduction from extracellular ligands.⁴² This is suggested by PEDF specific induction of IL-10 secretion by macrophages, of neurotrophic activity of neuronal cells, and of death in endothelial cells.⁴² However, how this signaling occurs within the cell remains unknown. Secondary messengers are essential in conferring and regulating the binding of extracellular ligands. By understanding this internal cellular machinery, we may better understand and employ this cell-signaling pathway for potential therapies in the future.

2.2. Comparison of unbiased approaches to identifying down-stream signaling proteins

Unbiased approaches to identifying down-stream signaling proteins are either based in genetic or proteomic strategies. Each has their own pros and cons. One traditional and common approach is through co-affinity purification followed by mass spectrometry (AP/MS). Affinity purification can be performed by either a protein complex or using immunoglobulins. Briefly, protein lysate is run through a column containing immobilized protein complex or immune-protein complex to allow binding to occur *in vitro*. Then, the entire complex is eluted off, purified and sent for mass spectrometry to identify the chemical. Mass spectroscopy can be optimized to identify non-known targeted chemicals, but is often easier when the predicted chemical is known (also known as

targeted analysis). This approach helps identify direct binding partners and can differentiate between homologous proteins. However, it performs this *in vitro* by forcing an interaction between two proteins that may not normally bind, resulting in false positives. Furthermore, this approach requires a highly concentrated, purified sample that may require complex purification schemes unsuitable for unstable proteins.

Another commonly used approach is yeast two-hybrid (Y2H) screening. This approach assumes that for two proteins to interact, they need to be in close proximity to each other. As such, one protein is fused to the Gal4 DNA-binding domain while a second protein is fused to the Gal4 activating domain. When both proteins near each other, the combination allows a functional Gal4 transcription factor that will transcribe a protein for yeast cells to survive in selective media. This approach can be complicated and incomplete as yeast do not retain the same post-translation modifications that occur in mammals. In addition, Y2H is prone to both high false negative and false positive rates as proximity may occur even though the proteins do not interact. This is exacerbated in membrane proteins and therefore would not be ideal for PLXDC1.

In contrast, genetic approaches in identifying important regulatory proteins has flourished after the whole genome-sequencing project. This allowed for the development of gene knockout strategies. Historically this was performed by short interfering RNA (siRNA) or small hairpin RNA (shRNA) pooled libraries, where whole genomes were down-regulated to determine which proteins were essential in the pathway. This has been partially supplanted with the CRISPR-Cas9, which is touted to provide targeted and specific gene deletions.^{44,45} Genetic approaches are advantageous compared to the aforementioned approaches as they can functionally evaluate multiple genes

simultaneously. However, redundant proteins can rescue the phenotype and mask real differences. In addition, genes that are essential to cell survivability may be missed. Regardless, these techniques allow for an unbiased approach to identifying novel proteins or genes involved in PLXDC1 signaling.

2.3. Mechanism of PLXDC1 receptor interaction

When PEDF is bound to PLXDC1, major transformational changes occur in PLXDC1 that permit receptor activation. PLXDC1 is known to exist in a homo- or hetero-dimer with its homolog PLXDC2. In this dimerized state, the receptor is not activated. This is mediated through two extracellular domains, domain A (amino acids 19-127) and domain D (amino acids 293-359). Domain A is considered the inhibitory domain while domain D is necessary for oligomerization.⁴² When domain A is deleted, the receptor takes on an active conformation allowing for downstream signaling. This activation mimics receptor activation when PEDF binds domain B, allowing a "scissoring" mechanism to occur between the two dimers (Figure 1). Understanding the mechanism of receptor activation provides us a way to evaluate receptor specific activation and endothelial cell death.

2.4. Detachment-induced cell death: anoikis

Detachment-induced cell death, also known as anoikis (*homelessness* in Greek) is a form of apoptosis induced by cell detachment from the extracellular matrix (ECM). Endothelial and epithelial cells require attachment and adherence to an underlying ECM and/or basement membrane for cell survival and proliferation.⁴⁶ Extracellular matrices are a complex network of macromolecules, including growth factors, collagen, or enzymes, that provide both biochemical

support and ligands for cell signaling. Disruption or alterations in this normal binding of cell surface receptors to the ECM can negatively affect cell survival. In cancer, cells may develop genetic mutations that allow cell survival despite detachment from the ECM, allowing for metastatic disease.⁴⁶ In contrast, endothelial cells are susceptible to cell death if unable to maintain a connection to the ECM. Preliminary studies (not shown) performed with a small molecule PLXDC1 agonist demonstrate the PLXDC1 activation causes detachment of the cell surface from the ECM *in vitro* (both mouse endothelial cells with and without a 3D matrix). Specifically, the initial morphological change prior to cell death *in vitro* is the "rounding" or "balling" up of endothelial cells which elongate and assemble cord-like vessels. These morphological changes *in vitro* are then followed by cellular detachment and cell death. Therefore, these findings suggest that PLXDC1-induced cell death may occur through anoikis.

In this chapter, we will describe how we identified down-stream signaling partners involved in PLXDC1-mediated anoikis with a genome-wide CRISPR-Cas9 knockout screen.

2.5. Materials and Methods

The reagents and equipment used in the experiments described in this chapter are listed in Table 2-1.

2.5.1. Cell culture and cell lines

Cell lines utilized were HEK293T human embryonic kidney cells and murine endothelial cells. Endothelial cells were either wild type or a transgenic, where they expressed human PLXDC1 cDNA under the endogenous promoter. Discussion of the knock-in transgenic construct is

described in Chapter 3. All cells were cultured at 37° Celsius at 5% CO₂ in DMEM with 10% fetal bovine serum with 100 U/mL penicillin/streptomycin. Serum free media conditions are defined as DMEM with 100 U/mL of penicillin/streptomycin. Maintenance cell sub-culturing was performed by passaging cells to a density of 50% by trypsinization (0.05% Trypsin-EDTA) every 3 days. HEK293T cells are utilized for receptor activation studies as they do not die in the presence of PEDF or a small molecule PLXDC1 agonist. However, presence of PEDF or a small molecule PLXDC1 agonist does cause downstream receptor dependent NF-kB activation. Murine endothelial cells were used for endothelial cell death assays as they naturally express PLXDC1 and die in the presence of PEDF or small molecule PLXDC1 agonist.

2.5.2. Genetic constructs

Full-length cDNA of PLXDC1 was cloned into a vector with a constitutively active promoter (CMV) and N-terminus Rim tag with an engineered secretion signal of alkaline phosphatase prior to the protein sequence. Full-length cDNA of downstream proteins was isolated from cDNA libraries of human or mouse tissues (endothelial, heart, liver, or brain) and HA tagged at the C-terminus followed by a stop codon. Rim tag is a 14-residue polypeptide (NETYDLPLHPRTAG)⁴⁷ and HA tag is a 9-residue polypeptide (YPYDVPDYA). The domains of PLXDC1 are: domain A (19-127), domain B (128-242), domain C (243-292), and domain D (293-359). Based on the above definitions, we made receptor constructs with different domain deletions. For PLXDC1 receptor activation, constitutively active promoters (CMV) caused a dominant negative effect; therefore, we cloned PLXDC1 into tet-inducible vectors with luciferase reporters. These constructs were engineered to have constitutively expressed with inducible PLXDC1 expression (Figure 2).

2.5.3. Tryptophan intrinsic fluorescence

To confirm direct binding between PLXDC1 and small molecule PLXDC1 agonist, we evaluated changes in intrinsic tryptophan fluorescence. We incubated 200 nM of recombinant PLXDC1 in PBS with varying concentrations of the small molecule PLXDC1 agonist for 10 minutes. Changes in fluorescence was detected with a Horiba Jobin Yoon fluorometer. Excitation wavelength was 280 nm. Fluorescent measurements were taken between 300 nm and 550 nm at 2 nm increments and an integration time of 0.1 seconds. Peak fluorescent intensity was compared over increasing concentrations of small molecule PLXDC1 agonist.

2.5.4. Genome-wide CRISPR Knockout (GeCKO)

Genome-wide CRISPR Knockout (GeCKO) was performed as previously described (Figure 2.1).^{44,48} Mouse GeCKO library was first obtained from Addgene from the Feng Zheng lab at MIT. The library composes 130,209 unique sgRNA with 6 sgRNAs targeting the 5' untranslated region of all genes in the mouse genome and is split into two halves (Library A and Library B). The one-vector lentiviral GeCKO system was used where one vector contained both the sgRNA and SpCas9 protein. The library was first expanded in Lucigen Endura electrocompetent cells onto 20 standard (10 cm round) ampicillin petri dishes. Transformation efficiency was calculated as the number of colonies exceeding 3×10^6 cells (50 x per sgRNA construct). Colonies were then harvested and maxi-prepped to isolate plasmid DNA.

Ten 10-cm dishes of 80-90% confluent HEK293T cells were then transfected with the GeCKO library lentivirus with helper plasmids (PMD2.G, psPAX2) in equal molar ratios (GeCKO: psPAX2:PMD2.G 4:2:1). HEK293T cells were then incubated in SFM for 48 hours. Virus was

harvested by spinning down cellular debris at 13,000xg for 10 minutes and removing supernatant. 8 µg/mL of polybrene was added as a transduction adjuvant. Combined, this was applied to resuspended murine endothelial cells in suspension at a multiplicity of infection (MOI) of <0.3 to permit individual gene alterations. 24-hours later, puromycin (0.5 µg/mL) was added and refreshed q3-4 days for selection. After 7 days, cells were split so that each condition received 7×10^7 cells. Cells were harvested at day 0 as a control. Selection conditions were either: 1) transiently transfection with full length PLXDC1, dA-PLXDC1, or dAC-PLXDC1 or 2) resuspended with a small molecule PLXDC1 agonist at 10-20 µM or equivalent amount of DMSO. For transient transfections, G418 was added to 300 ng/µL 24 hours later and cells were harvested 3 days after transfection. For small molecule PLXDC1 agonists, cells were harvested 48 hours after resuspension.

Harvested cells were spun down and genomic DNA was isolated (Invitrogen). PCR amplification was performed with pooled next generation sequencing (NGS) primers. NGS primers were designed to amplify the sgRNA target region with Illumina adaptor sequences. To reduce biased PCR amplification, 24 amplification cycles and 10 different forward primers were used with one reverse primer that was barcoded. Samples were then sequenced by Illumina HiSeq with 80- cycles of read 1 (forward) and 8 cycles of index 20% PhiX control was spiked in with a coverage of >100 reads per sgRNA.

To determine top candidate genes, genes were first sorted by GO terms for cytoplasm (GO:0005737), cytosol (GO:0005829), or plasma membrane (GO:0005886). Genes were then

compared by enrichment (or numerical counts). Genes with the largest enrichment between control and treatment were identified and subsequently evaluated.

2.5.5. Functional cell assays:

2.5.5.1. Cell receptor activation assay

To determine whether antibody binding to the receptor causes activation, we have developed a receptor activation assay based in HEK293T cells. PEDF is known to cause an increase of transcription in NF- κ B. Therefore, we utilized a commercially available plasmid that has five copies of an NF- κ B response element that drives the transcription of luciferase. This is co-transfected with a tet-inducible PLXDC1.

We first split HEK293 cells 1:4 into a 96 well dish. We then heterologously express the inducible PLXDC1 construct, NF- κ B construct, and empty vector or integrin beta-1 construct in a 1:1:1 ratio using jetPrime. After 4-6 hours, the cells are washed with HBSS and replaced with serum free DMEM with 10 μ M of a small molecule PLXDC1 agonist. 48 hours later, cells are lysed (25 mM of Tris-phosphate, 2 mM of DTT, 2mM of 1,2-diaminocyclohexane-N,N,N',N'-tetraacetic acid, 10% glycerol, 1% Triton-100) for 10 minutes, placed in the POLARStar OMEGA plate reader, luciferase substrate added and luminescence read.

2.5.5.2. Cell adhesion assay

To determine the if a small molecule PLXDC1 agonist inhibits normal endothelial cell adhesion, immortalized murine endothelial cells were trypsinized and resuspended in serum free media with a small molecule PLXDC1 agonist at 10 μ M. After four hours, cells are evaluated under light

microscopy to determine their ability to adhere the plastic well. Twenty-four after initial resuspension, cells either undergo MTT assay (described below) or dual staining with fluorescein diacetate and propidium iodide to determine cell viability.

2.5.5.3. Endothelial cell death assay

To evaluate cell death *in vitro*, mouse endothelial cells that are known to express PLXDC1 and die to presence of PEDF were utilized. These cells were chosen as this is the targeted cell *in vivo* and recapitulates the downstream signaling cascade. Mouse endothelial cells were trypsinized, washed, and resuspended in serum free DMEM. Alternatively, mouse endothelial cells were split 1:3 the day before a small molecule PLXDC1 agonist was added. Small molecule PLXDC1 agonist was added at 10 μ M and cell death was evaluated 24 or 48 hours after resuspension. Cell death was quantified with an MTT assay or fluorescent dyes.

For MTT assay, cells are incubated in MTT (3-[4,5-dimethylthiazol-2-yl]-2,5-diphenyltetrazolium bromide) reagent at a final concentration of 100 μ g/ml for 30 minutes at 37° Celsius. Media was then removed and cells were lysed into 50 μ L of DMSO. Absorbance was then read at 550 nm in the POLARStar Omega plate reader.

To determine cell viability by fluorescent dyes, fluorescein diacetate and propidium iodide were used to determine alive and dead cells respectively. Fluorescein diacetate was added to a final concentration of 0.5 μ M and propidium iodide was added to a final concentration of 15 μ M. Cells were then incubated in 37° Celsius. Cells were then immediately imaged.

2.5.6. siRNA-mediated knockdown

To evaluate positive genes identified in the GeCKO screening, transient siRNA infections were performed. All siRNAs were purchased from Dharmacon, Inc. and were the ON-TARGETplus SMARTpool siRNAs. The following specific catalog numbers and genes are as follows: Ilk (L-040115-00-005), Mapk6 (L-040133-00-0005), Itgb1 (L-040783-01-0005), Slc7a5 (L-041166-01-0005), Gbp6 (L-041286-00-0005), Itgav (L-046779-01-0005), Cdc42ep4 (L-049988-01-0005), Cdc42ep5 (L-063228-01-0005), RhoA (L-042634-00-0005), Tmem17 (L-058017-01-0005), Ms4a13 (L-054409-01-0005), Pgg1b (L-055452-01-0005), Gtpbp6 (L-064062-01-0005), Antxr2 (L-065917-01-0005), Nkiras1 (L-065228-01-0005), Src (L-040877-00-0005), Ptk2 (L-0410990-00-0005), and Krt7 (L-063818-01-0005). Control siRNA was from Invitrogen, which showed cell death. siRNA was transfected through reverse transfection using RNAiMAX in antibiotic free culture medium (OptiMEM) at 50 nM concentration with a cell splitting ratio of 1:3. To achieve a high transfection rate and knockdown effect, reverse transfection was performed twice consecutively following the manufacturer's protocol. At 48 hours after transfection, the cells were reverse transfected again using the same siRNA for the second round of knockdown. Functional assays were performed 48 hours after the second round of reverse transfection.

2.5.7. Western blot Analysis

Western blot was performed utilizing 1 µg of antigen per lane. Gel electrophoresis was performed on a 12% SDS-PAGE gel and transferred onto a nitrocellulose membrane. Primary antibody for phosphorylated focal adhesion kinase (Tyr397) was obtained from Cell Signaling Technologies (Catalog #8556T) and used at a 1:5000 dilution. Beta-tubulin loading control antibody was obtained from ThermoFisher Scientific (Catalog #MA5-16308) and used at 1:5000 dilution.

LiCOR IRDye 800CW secondary anti-Rabbit IgG and IRDye 680LT secondary anti-Mouse IgG were used at 1:10,000 dilution.

2.5.8. Co-purification: co-immunoprecipitation and western blot

Rim-tagged proteins were purified using the anti-Rim antibody- conjugated to CNBr-activated Sepharose 4 Fast Flow beads (Amersham/GE Healthcare). Briefly, cells were washed once with HBSS and lysed in well with 1% Triton X-100 in HBSS and protease inhibitors for 30 min on ice. Cell lysate was spun at 16,000×g, 4°C for 10 min to remove insoluble materials. Cell lysate was applied to anti-Rim antibody conjugated beads, and rotated for 4 hours at 4°C. The beads were washed three times using 0.1% Triton X-100 in HBSS by spinning down at 1000×g for 30 s and eluted in 0.1% Triton X-100 in 0.1 M Glycine, pH = 2.3 for 15 min at room temperature. Tris (pH 9.5) was added to 0.1 M to neutralize the elution before the samples were analyzed. HA-tagged proteins were detected using a monoclonal anti-HA antibody. To determine interaction between beta-integrin and PLXDC1, Rim-tagged full length and deletional PLXDC1 constructs were co-transfected with HA-tagged integrin beta 1 (ITGB1) at equal molar ratio. Co-purified receptors were detected either by anti-HA antibody.

2.6. Results

2.6.1. Small molecule PLXDC1 agonist binds to PLXDC1 and causes conformational change

To determine whether small molecule PLXDC1 agonist binds and interacts with PLXDC1, we evaluated the change in intrinsic tryptophan fluorescence with increasing concentrations of small molecule PLXDC1 agonist. Depending on the steric orientation of tryptophan, when excited with

280 nm wavelength light, it emits an autofluorescence ranging from 300-550 nm. In the presence of increasing concentrations of PLXDC1 small molecule agonist, tryptophan fluorescent quenching is noted (Figure 2-4). This tryptophan quenching is noted to saturate at 30 nM. After performing a best-fit line, the equilibrium dissociation constant (KD) was calculated to be approximately 15 nM.

2.6.2. Small molecule PLXDC1 agonist causes anoikis, detachment induced cell death

Resuspension of endothelial cells with a small molecule PLXDC1 agonist prevents cell adhesion compared to control at 24 hours (Figure 4). In confluent endothelial cell dishes, addition of a small molecule PLXDC1 agonist causes endothelial cells to lose their adhesive properties as they "balled up". These morphological changes caused the cells to detach, confirmed by a lack of cell adhesion that ultimately led to apoptosis.

To confirm cells were undergoing anoikis, downstream signaling proteins were evaluated. Normally, beta-catenin is membrane bound and nuclear; however, in the presence of a small molecule PLXDC1 agonist, beta-catenin re-localized to a peri-nuclear organelle or cytosolic, suggesting proteasomal degradation. Separately, focal adhesion kinase (FAK) phosphorylation was evaluated which showed decreased phosphorylation of FAK compared to control. This supports anoikis as the mechanism of PLXDC1-mediated cell death.

2.6.3. Genome-wide knock-out screening identifies genes involved in PLXDC1 mediated cell death

To unbiasedly identify novel downstream genes involved in PLXDC1-mediated cell death, we utilized two different known receptor activating mechanisms. The first was a small molecule PLXDC1 agonist (Figure 4) and the second was ectopic expression of the domain A deleted PLXDC1 receptor (Figure 5). Both methods showed significant cell death (Figure 4 and 5) compared to controls but with a small minority of cells gaining a selective advantage after positive selection. These cells had their genomic DNA isolated. Deep sequencing revealed a wide assortment of enriched proteins. Genes identified were selected based on cell location (GO terms of membrane or cytosolic proteins). Highest enriched genes were then excluded if they were related to cell division or directly with apoptosis as these would provide selective growth advantage unrelated to the PLXDC1. Genes identified previously by LC/MS or were found to be highly enriched by GeCKO screening are presented in Figure 12.

2.6.4. PLXDC1-mediated cell death depends on ITGB1

We performed siRNA screening on endothelial cells of the top identified genes. We utilized a small molecule PLXDC1 agonist as the positive selection criterion and evaluated which siRNAs were effective in preventing anoikis and cell death. Amongst those, we found that siRNA knockdown of ITGB1 prevented PEDF mediated anoikis. ITGB1 is essential in the binding of endothelial cells to the extracellular matrix and is one of the primary integral membrane proteins involved with anoikis. To confirm ITGB1 importance in PLXDC1 signaling, we found that in the presence of a small molecule PLXDC1 agonist, PLXDC1 mediated NF- κ B transcription increases in the presence of ITGB1 (Figure 11). Independently, ITGB1 was found by affinity chromatography/mass spectroscopy performed in the lab prior to be a binding partner with PLXDC1. This was established by co-immunoprecipitation between ITGB1 and full length and

deletional constructs of PLXDC1 indicates that ITGB1 binds PLXDC1 in the D domain. In addition, the activated PLXDC1, where the A domain is deleted, shows increased binding to ITGB1 (Figure 12).

2.7. Discussion

In this chapter, we describe two key components of PLXDC1-mediated cell death. We first demonstrate that in the presence of a small molecule PLXDC1 agonist, endothelial cells are not able to attach to the extracellular matrix and ultimately die. This pathway is consistent with anoikis or detachment induced cell death. Second, we utilized genome wide CRISPR-Cas9 knock out screening, coupled with affinity chromatography and mass spectroscopy, to identify downstream signaling proteins. To phenotypically evaluate which genes were essential in the development of PLXDC1 mediated cell death, we perform transient siRNA knockdown and found that ITGB1 prevented PLXDC1 mediated cell death. This further confirms the development of anoikis as the primary cell death pathway of PLXDC1.

The findings in this paper suggest that PLXDC1 mediated cell death is consistent with anoikis. First, the addition of a small molecule PLXDC1 agonist prevents cellular adhesion when cells are placed in suspension. Second, the addition of a small molecule PLXDC1 agonist in confluent endothelial cells shows that exposed endothelial cells begin to "ball"-up, detach, and die. This is further confirmed by the decreased phosphorylation of FAK and re-localization of beta catenin in a peri-nuclear organelle or cytoplasm, likely suggesting proteasomal degradation.⁴⁹ Third, resistance to a small molecule PLXDC1 agonist induced cell death by siRNA knockdown of ITGB1 suggest its necessity in PLXDC1-mediated cell death. Fourth, ITGB1 co-purification with

PLXDC1 confirms that the two proteins interact. Increased binding between ITGB1 and A domain deleted, or activated, PLXDC1 receptor supports this hypothesis. Combined these findings provide evidence that PLXDC1 cell death occurs through anoikis.

Targeting anoikis is not a novel therapeutic approach in angiogenesis. In 1997, a cyclic peptide called Cilengitide showed nanomolar affinities for integrin $\alpha v\beta 5$ and $\alpha 5\beta 1$ and was patented with Merck.⁵⁰ The proposed mechanism was twofold: to prevent angiogenesis and reduce metastatic potential of cancer cells, thereby having both a primary and synergistic role with chemotherapy.⁵⁰ In pre-clinical trials, Yamada et al. showed tumor inhibition in nude mice injected with human glioblastoma.⁵¹ This success was continued in promising phase 1 and 2 clinical trials.⁵² Unfortunately, in a multicentric phase 3 clinical trial, no improvement in overall survival from addition of Cilengitide to standard of care was noted.⁵³ However, the failure of Cilengitide does not indicate that endothelial cell anoikis is not a viable anti-angiogenic pathway, but rather may highlight the limitations of targeting integrins with cyclic peptides in treating primary brain cancer. First, redundancy of integrins may be present, preventing anoikis *in vivo*. Second, cyclic peptides have sub-optimal pharmacokinetic profiles, such as short half-lives, that may be insufficient to be therapeutically active. In addition, systemic administration of a drug targeting glioblastoma multiforme may have further reduced drug availability as it needs to cross the blood brain barrier.⁵⁴ Targeting PLXDC1, which causes cell death in endothelial cells through anoikis, may be more potent than direct integrin targeting. This may be due to differential conformational changes unique to PLXDC1 that small cyclic peptides could not achieve. Furthermore, utilizing antibodies overcomes the pharmacokinetics and dynamics that limit peptides.

Genome-wide knockout screening identified novel genes involved in PLXDC1-mediated cell death. This wide range of genes involved actin and cytoskeletal proteins, secondary messengers associated with small GTPases, non-receptor tyrosine kinases, and integral membrane proteins. Further confirmation of these genes is necessary to validate their importance in PLXDC1-mediated cell death. However, genes involved with anoikis were notably absent. This may be because these genes are essential for cell survival. In addition, genes identified by affinity chromatography / mass spectrometry were not amongst the highest enriched genes. This demonstrates the complementary nature of these two approaches where proteomic approaches are able to identify direct binding partners but cannot test functional importance; in contrast, genetic approaches can screen functional necessity of each gene but cannot identify essential genes.

In attempt to leverage this endothelial cell death pathway, we are developing novel therapeutic agents. These agents are innovative as they would be the first therapeutic antibody that activates a cell-surface receptor and kills endothelial cells in pathogenic blood vessels. Such an antibody does not exist in the clinic as all existing therapeutic antibodies in the clinic are neutralizing antibodies. Furthermore, current anti-angiogenic biologic drugs in the clinic (e.g. bevacizumab or aflibercept) can only partially inhibit blood vessel growth, but cannot kill pathogenic blood vessels. This incomplete treatment explains the need for repetitive injections and that have limited efficacy in cancer therapy. This leaves a gap in therapy that we will try to address in the next chapter.

Table 2-1 List of reagents and equipment

	Material/Equipment	Description	Manufacturer
Reage	Anti-Beta Tubulin	Beta-tubulin loading control antibody (Catalog #MA5-16308)	ThermoFisher Scientific
	DMEM	Dulbecco's Modified Eagles Medium	Corning, cellgro

DMSO	Dimethyl sulfoxide	Corning, cellgro
Endura Electrocompetent Cells	Endura electrocompetent cells	Lucigen, Inc.
Anti-phospho-FAK (Tyr397)	Monoclonal Anti-phospho-FAK antibody (Catalog #8556T)	Cell Signaling Technologies
FBS	Fetal Bovine Serum	Corning, cellgro
Fluorescein Diacetate	Alive cell fluorescent dye	Sigma
G418, Geneticin	Geneticin Selective Antibiotic	Gibco, Life Technologies
GeCKO v2 CRISPR KnockOut 2.0	Genome-scale CRISPR Knock-Out Library	Addgene, Inc
HBSS	Hank's Balanced Salt Solution	Hyclone
IRDye 800CW Ab	IRDye 800-conjugated goat anti-rabbit IgG antibody	Li-Cor
IRDye 680CW Ab	IRDye 680-conjugated goat anti-mouse IgG antibody	Li-Cor
jetPRIME	DNA transfection reagent	Polyplus-transfection
Luciferase assay system	n/a	Promega
monoclonal α -Rim	Monoclonal anti-Rim antibody	n/a
MTT reagent	N/a	Life Science Research Products
Nitrocellulose membrane	n/a	Maine manufacturing
PBS	Phosphate Buffered Saline	Corning cellgro
Penicillin/Streptomycin	Penicillin/streptomycin (10,000 U/mL)	Gibco, Life Technologies
Polybrene (hexadimethrine bromide)	Transduction adjuvant reagents	EMD Millipore
polyclonal α HA	Polyclonal anti-HA antibody	Genemed Synthesis
Propidium iodide	Cell death fluorescent dye	Sigma
PureLINK Genomic DNA Mini Kit	Genomic isolation kit	Thermo Fisher Scientific
Sepharose beads	CNBr-activated Sepharose 4 Fast Flow beads	Amersham, GE Healthcare
Triton X-100	Triton X-100 surfactant	Omnipur, Millipore
Trypsin	0.05% trypsin	Corning, cellgro
Trypsin Inhibitor	DTI, defined trypsin inhibitor	Gibco, Life Technology

Equipment	96-well plate	96-well, flat and clear bottom	Genesee Scientific
	HiSeq 2500	Ultra-high-throughput genome sequencer	Illumina
	Infra-red Imager	n/a	Li-Cor
	Nikon Eclipse Ti	Fluorescent Inverted Microscopy	Nikon
	POLARstar Omega	n/a	BMG Labtech

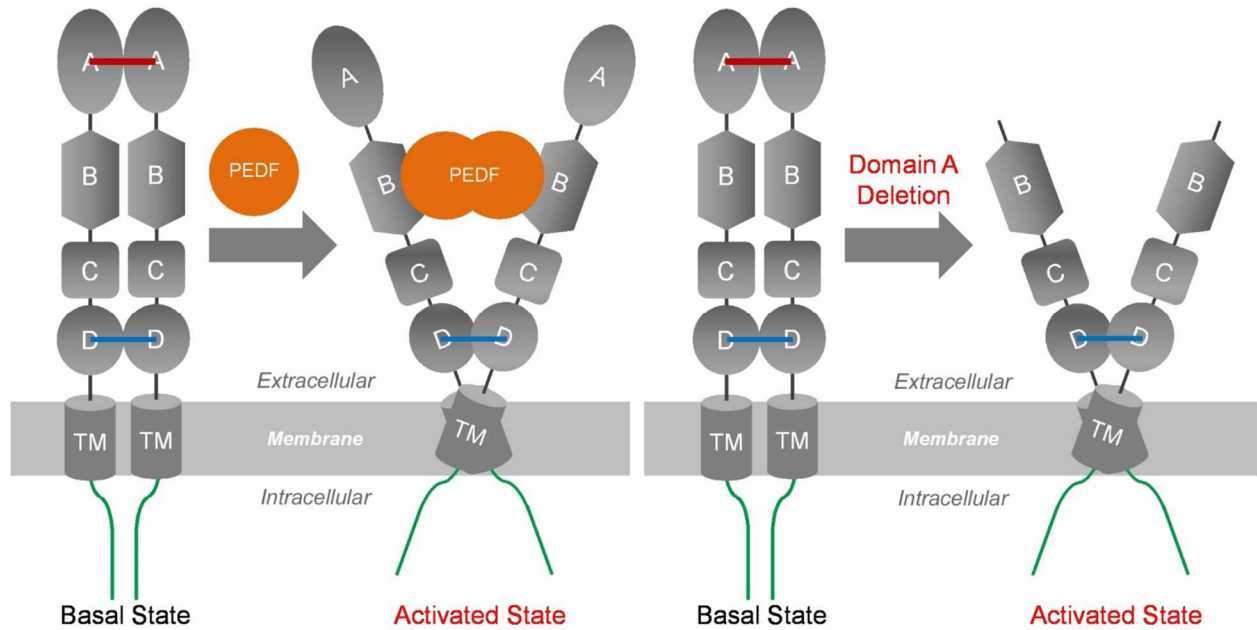


Figure 2-1. Proposed mechanism of PLXDC1 activation

In the basal state, PLXDC1 is a homodimer. However, when PEDF binds domain B of PLXDC1 or if the A domain is deleted, the receptor is activated, allowing for signal transduction.

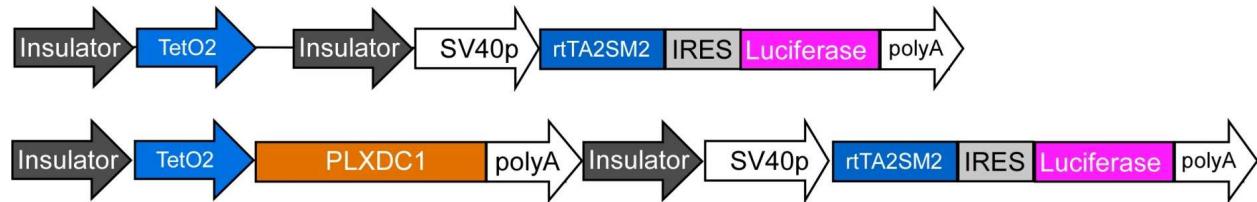


Figure 2-2. Inducible PLXDC1 constructs

Vector maps of the inducible control (top) or PLXDC1 (bottom) constructs utilized to evaluate PLXDC1-mediated receptor activation.

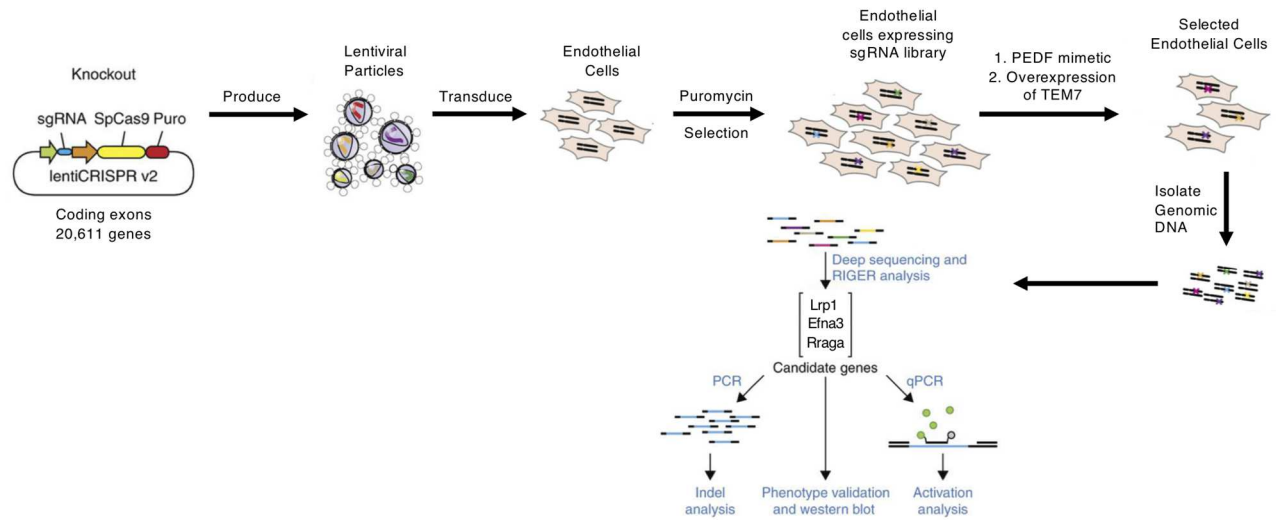


Figure 2-3. Genome-wide CRISPR-Cas9 knockout screening approach

Cartoon schematic of the GeCKO screening performed. A library of lentivirus targeted against the 5' untranslated region of 20,611 genes in the mouse genome was produced and transduced in an immortalized endothelial cell line. Cells are subsequently selected by puromycin and then positively selected after PLXDC1 overexpression or small molecule PLXDC1 agonist treatment.

Genomic DNA is then isolated and deep sequencing was performed to identify potential candidate genes.

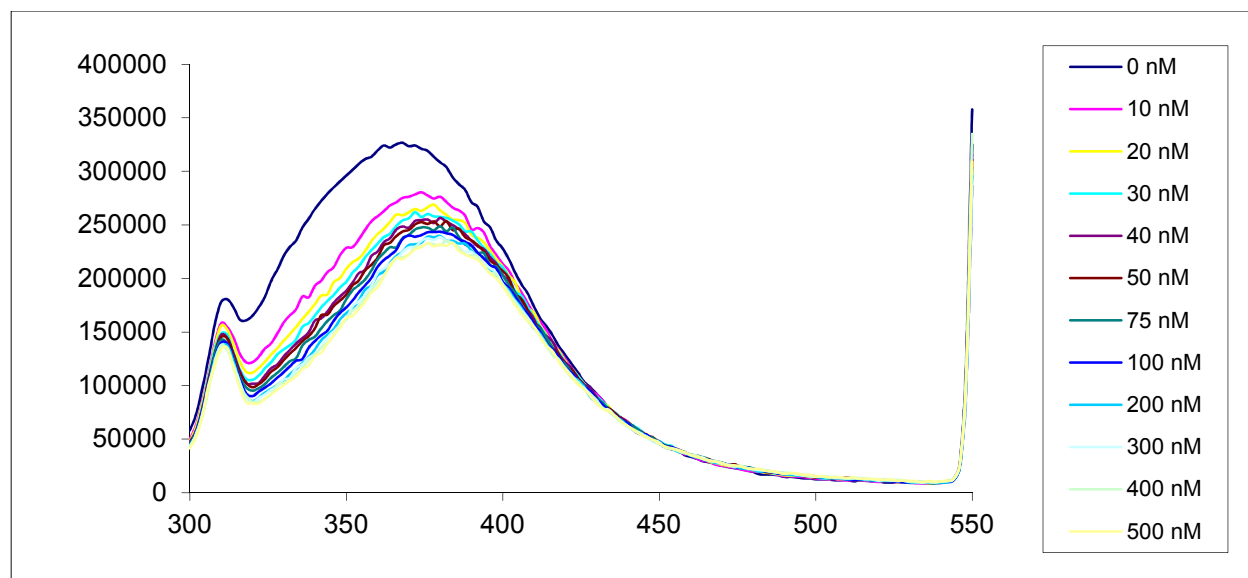


Figure 2-4 Small molecule PLXDC1 agonist binds to and causes PLXDC1 conformational change

Intrinsic tryptophan fluorescence was measured between recombinant PLXDC1 and increasing concentrations of small molecule PLXDC1 agonist. With increasing concentrations of small

molecule quenching of the intrinsic tryptophan fluorescence was noted that saturated around 15 nM.

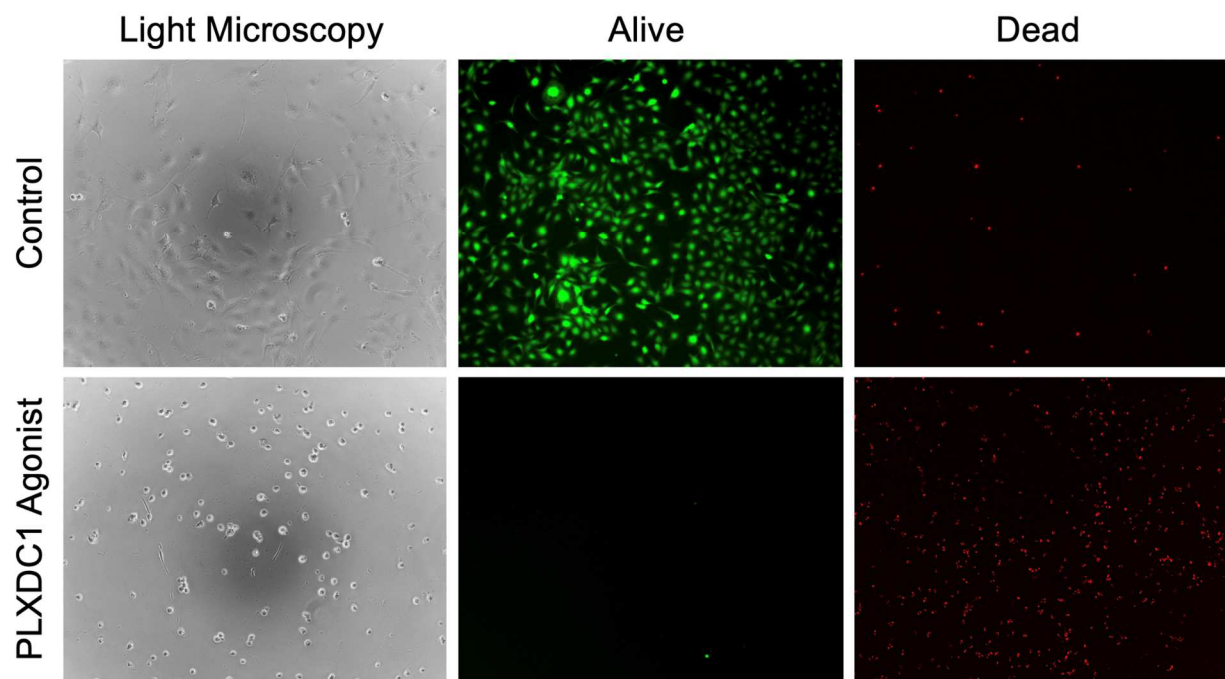


Figure 2-5. Small molecule PLXDC1 agonist induces anoikis in endothelial cells

Inhibition of cell adhesion and subsequent cell death at 24 hours with 10 μ M of a small molecule PLXDC1 agonist.

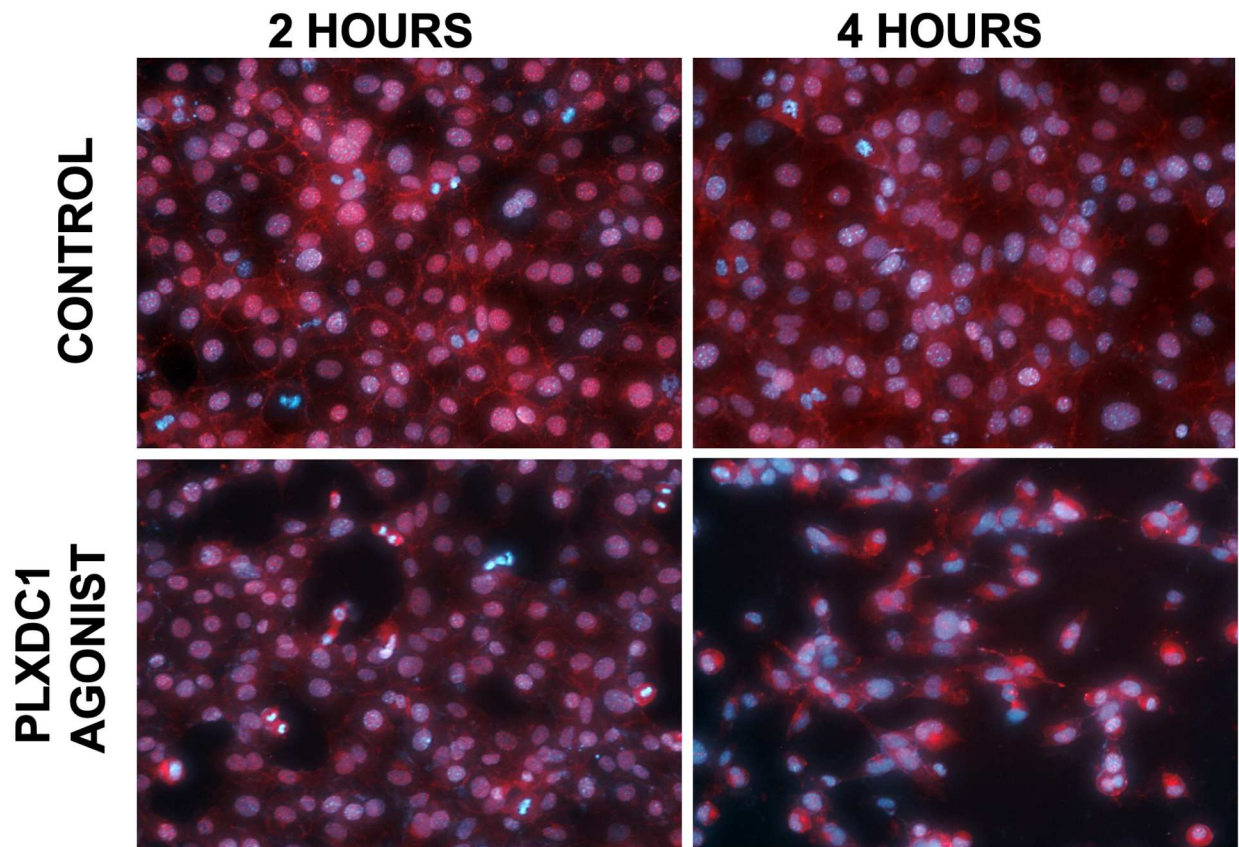


Figure 2-6. Beta-catenin localization with a small molecule PLXDC1 agonist treatment

Immunocytochemistry of mouse endothelial cells treated with control or a small molecule PLXDC1 agonist (10 μ m) shows cell death with re-localization of membrane bound beta-catenin to a cytoplasmic distribution, suggesting potential proteasomal degradation.

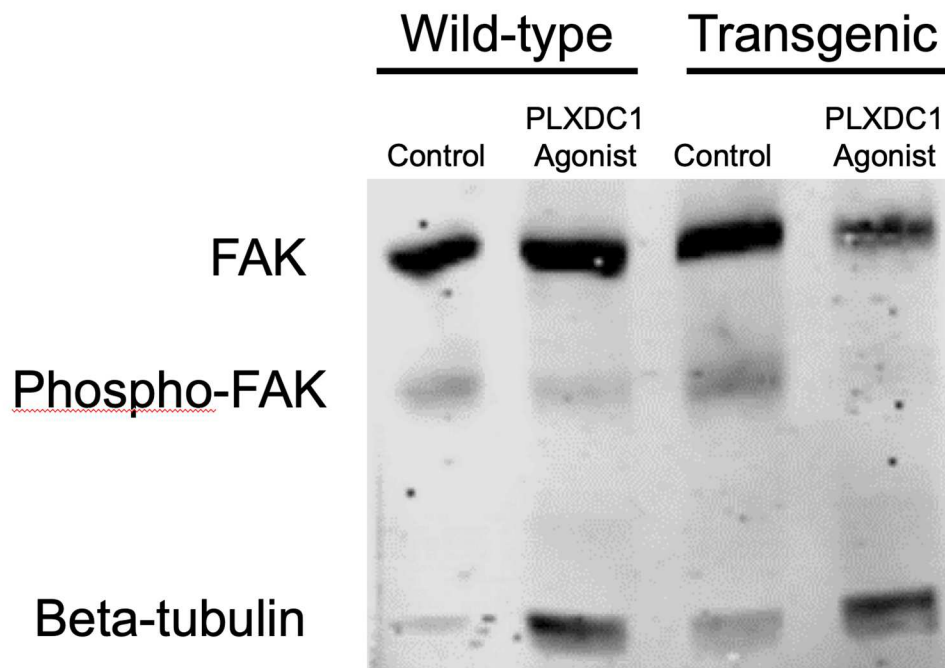


Figure 2-7. Phosphorylation of focal adhesion kinase in small molecule PLXDC1 agonist treatment

Western blot analysis of phospho-focal adhesion kinase (FAK), a downstream signaling protein of integrin beta-1 mediated anoikis, shows decreased phosphorylation of phospho-FAK at 4-hour incubation. This occurred in both wild-type mouse endothelial cells and transgenic endothelial cells that express human PLXDC1.

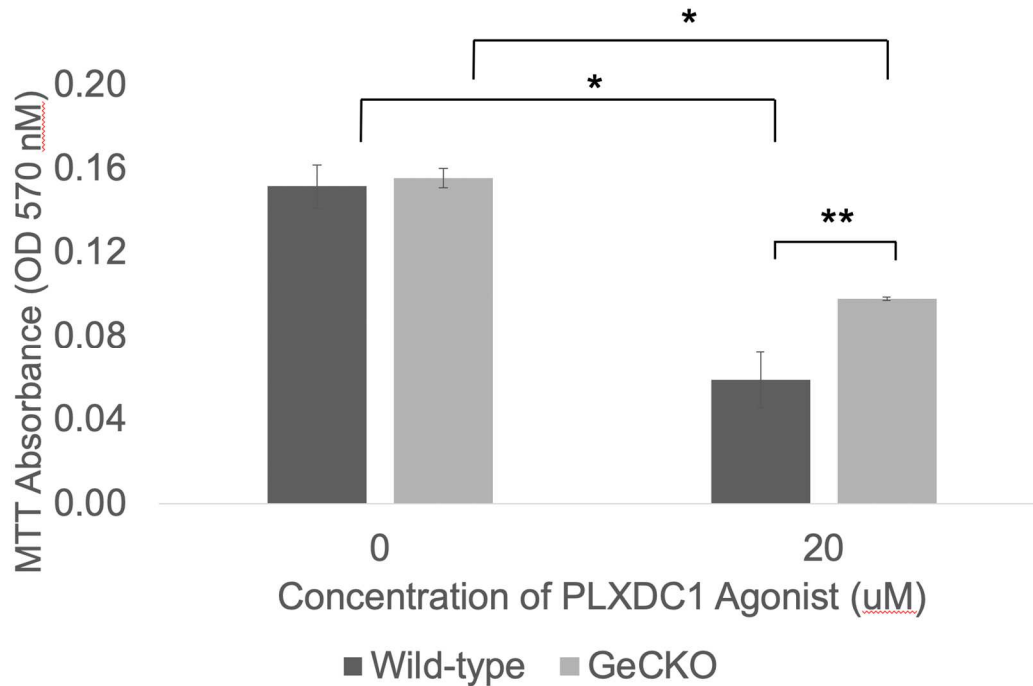


Figure 2-8. Genome wide CRISPR-Cas9 Knockout (GeCKO) provides selective advantage in small molecule PLXDC1 agonist treatment

MTT assay between wild-type and GeCKO library expressing endothelial cells. In the presence of a small molecule PLXDC1 agonist, there is survival of selective endothelial cell clones, suggesting knockdown of genes involved in endothelial cell death induced by a small molecule PLXDC1 agonist.

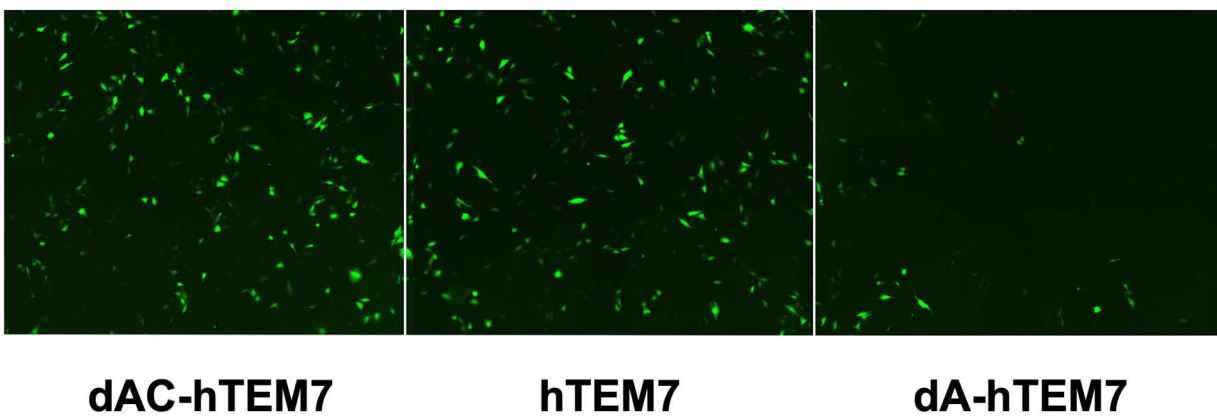
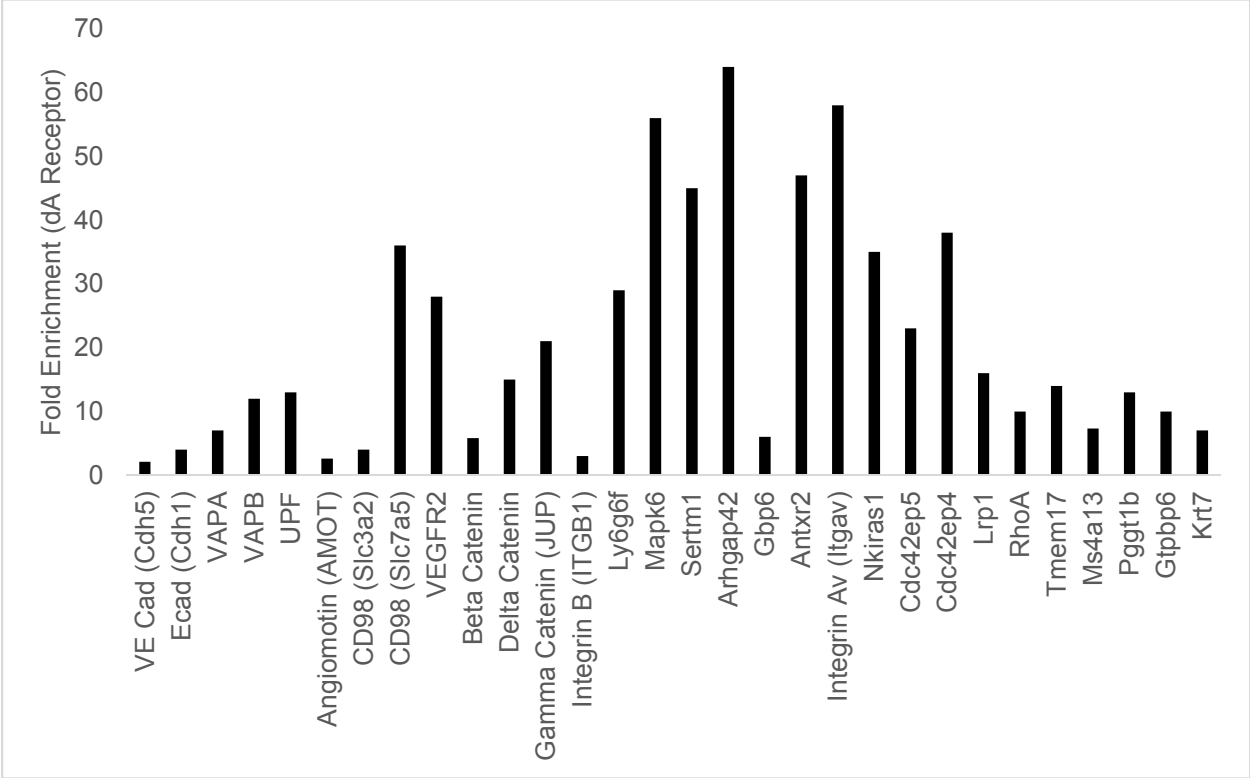


Figure 2-9. Expression of activated PLXDC1 (TEM7) receptor causes cell death

Co-expression of EGFP with full length or deletional constructs of PLXDC1 (human TEM7) indicate toxicity to endothelial cells with the activated receptor (dA-hTEM7) as compared to full-length or truncated receptor from the A to C domain (dAC-hTEM7).



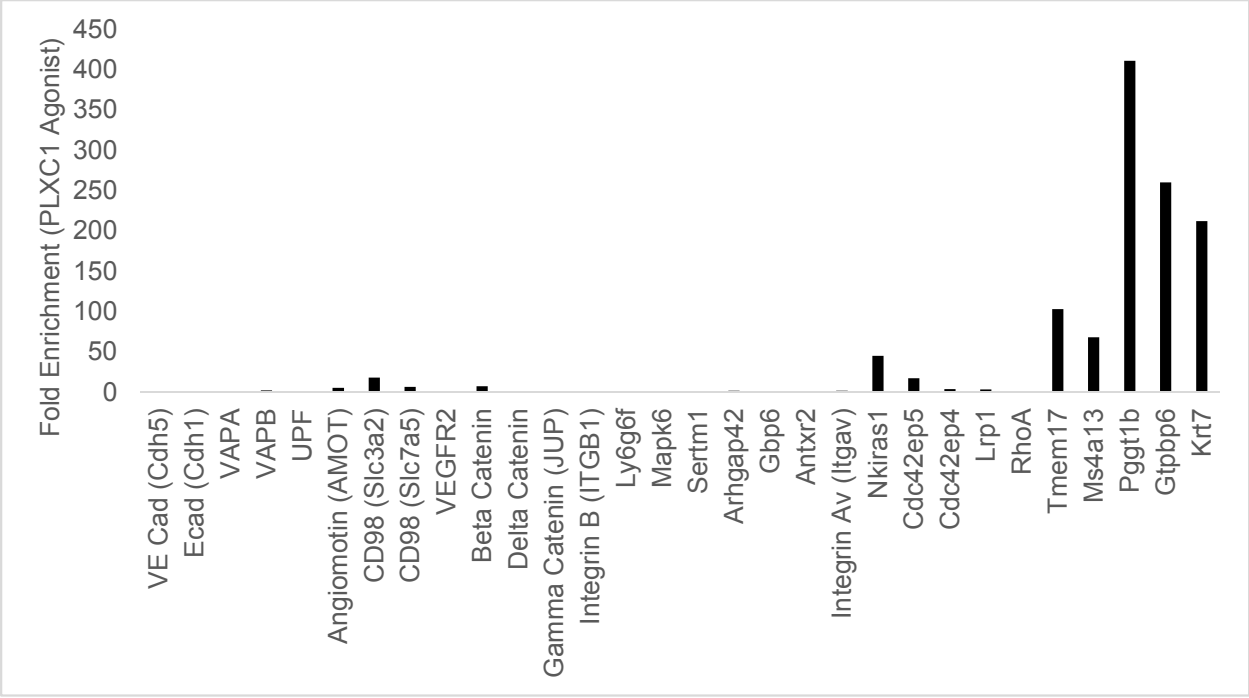


Figure 2-10. Genome wide CRISPR-Cas9 Knockout (GeCKO) screening

A wide variety of membrane and cytosolic proteins show significant fold enrichment in endothelial cells treated with a small molecule PLXDC1 agonist or expressing the activated receptor.

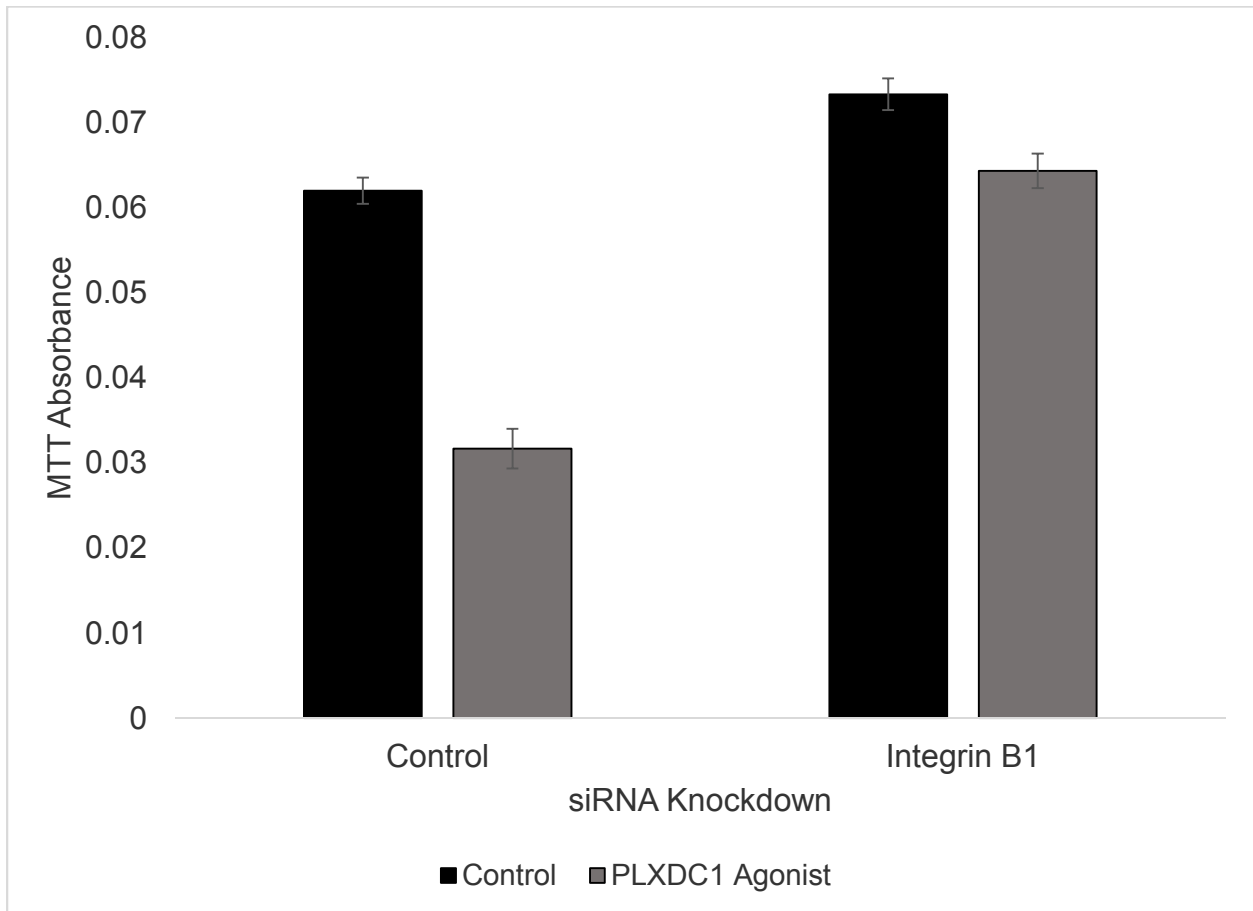


Figure 2-11. siRNA knockdown of ITGB1 inhibits small molecule PLXDC1 agonist cell death

Knockdown of ITGB1 shows inhibition of cell death from a small molecule PLXDC1 agonist (10 μ M) at 24-hours by MTT assay.

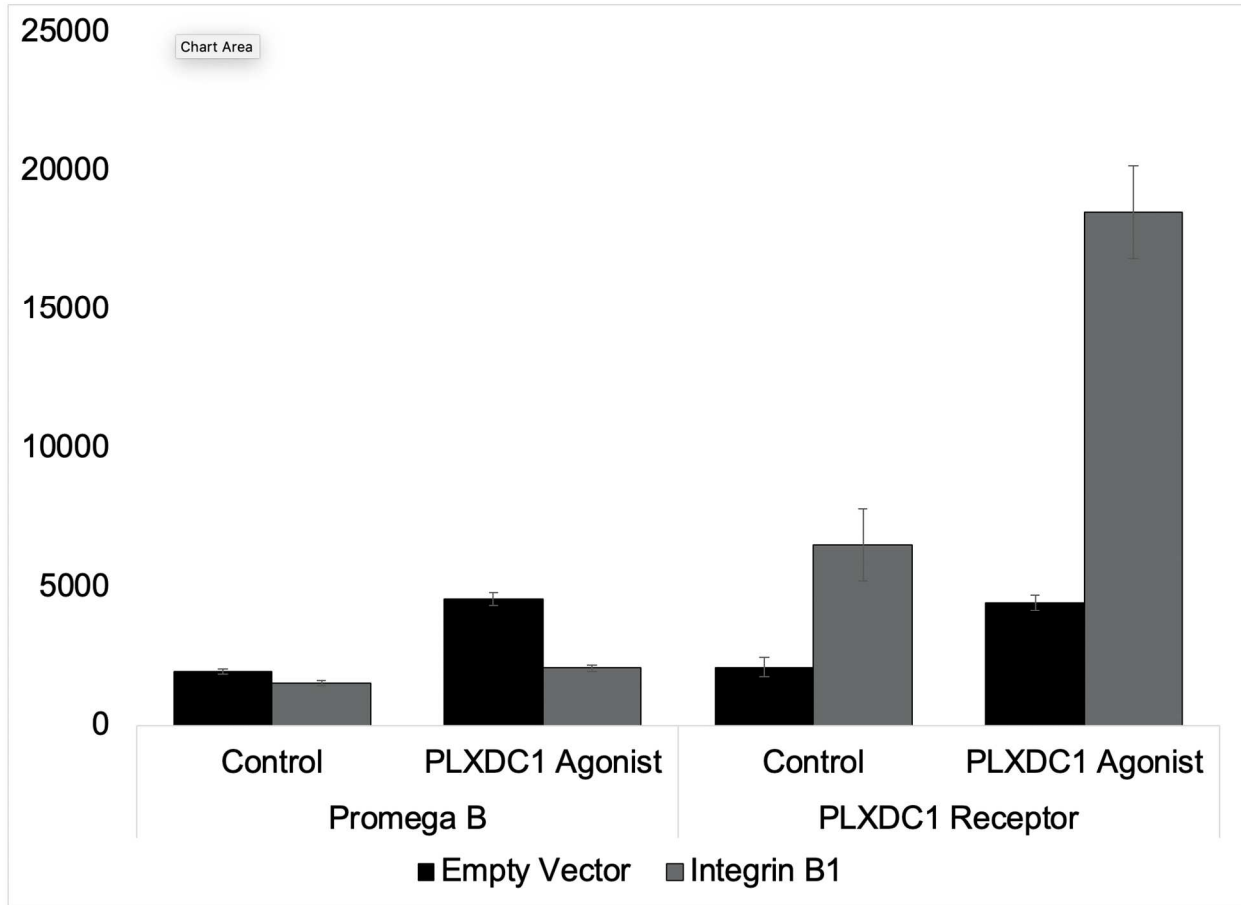


Figure 2-12. PLXDC1 specific receptor activation is enhanced with ITGB1 co-transfection

Small molecule PLXDC1 agonist was added at 10 μ m to induce receptor specific induction of NF-kB transcription. Presence of a small molecule PLXDC1 agonist in a luciferase control vector with and without ITGB1 showed no induction of NF-kB transcription. However, presence of ITGB1 with PLXDC1 caused a significant increase in NF-kB transcription that was further increased with addition of a small molecule PLXDC1 agonist.

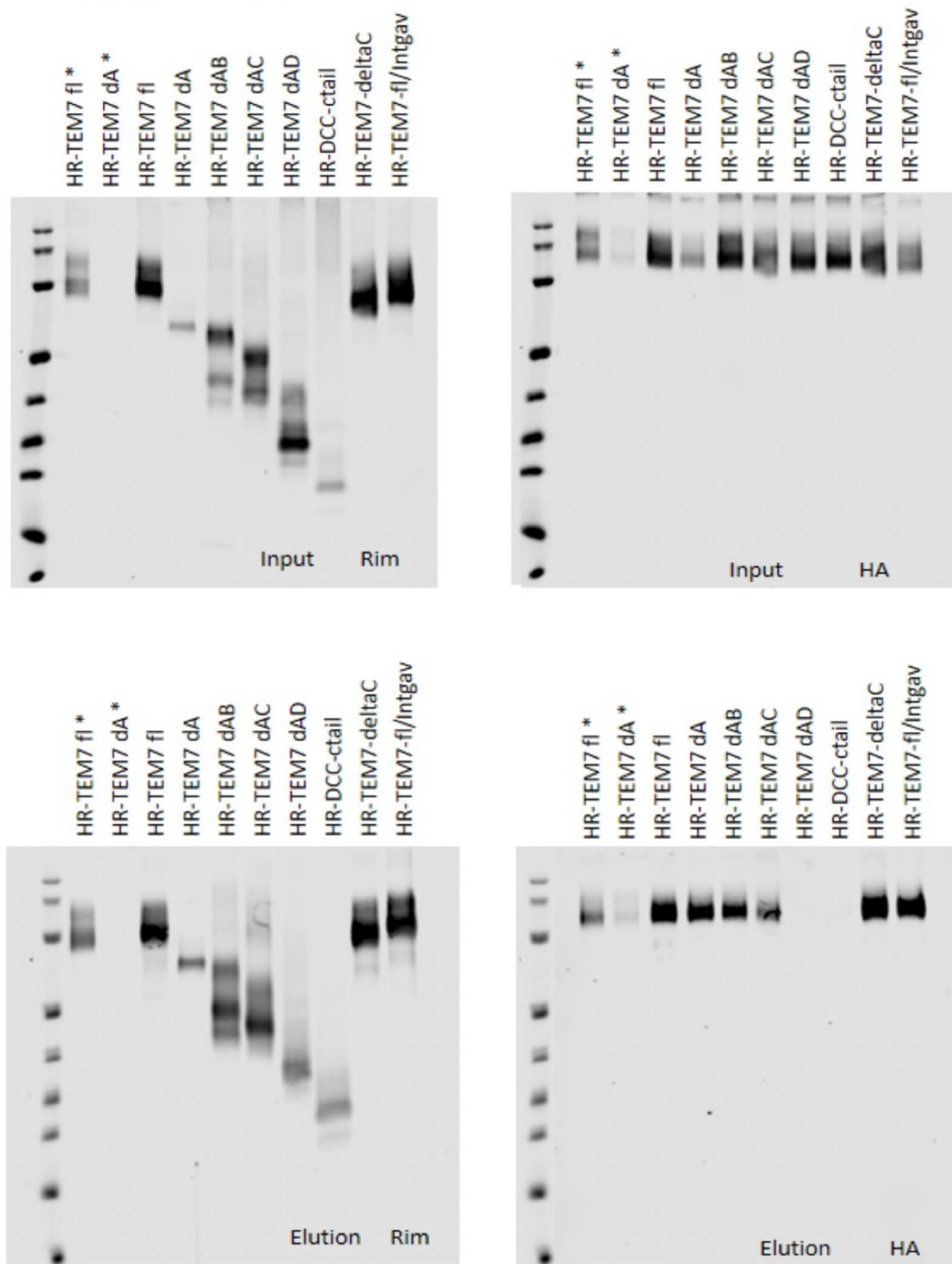


Figure 2-13. Co-immunoprecipitation of Rim-tagged full length and deletional constructs of PLXDC1 (TEM7) with ITGB1

Co-immunoprecipitation between full length and deletional constructs of PLXDC1 (TEM7) and ITGB1 demonstrates binding of ITGB1 to the D domain of PLXDC1 (TEM7). In addition, the

activated PLXDC1 (TEM7) receptor (domain A deleted), shows enhanced co-immunoprecipitation with ITGB1 compared to full length PLXDC1 (TEM7).

CHAPTER 3: DEVELOPMENT OF A THERAPEUTIC ANTIBODY THAT TARGETS PLXDC1

3.1. Introduction of modern therapeutic antibodies and potential significance

From the first monoclonal antibody approved by the FDA in 1986, therapeutic monoclonal antibodies have come to the forefront of modern medicine becoming a \$20 billion-dollar industry as of 2006.⁵⁵ This is in large part due to the high specificity, preferred side-effect profile, longer half-life, ability to scale, and reduced need for extensive structure-activity relationship analysis that plagues small molecules.⁵⁶ With such high specificity, monoclonal antibodies leverage advances in genetic sequencing and translational basic medical science to deliver targeted personalized medicinal therapies. Now with over 30 monoclonal antibodies FDA approved and success in a wide-variety of conditions, including cancer and rheumatologic disease, biologic therapies have become a commonplace and powerful tool in the therapeutic armamentarium of clinicians.⁵⁷

3.2. Current strategies for monoclonal antibody development

The two strategies currently utilized to develop and produce monoclonal antibodies for drug discovery are hybridoma and phage display. Hybridoma technology was first described in 1975 by Kohler and Milstein where they produced anti-sheep red blood cell antibodies by fusing lymphocytes isolated from mice spleens with myeloma cells.⁵⁸ This laid the groundwork for the "traditional" hybridoma approach, which awarded them the Nobel Prize in Physiology/Medicine in 1984. In the hybridoma approach, mice are immunized with a purified antigen or peptide sequences causing the mouse immune system to generate specific antibodies against a specific

epitope on the immunized antigen.⁵⁹ These cells are then fused with immortalized myeloma cells that lack both the hypoxanthine-guanine-phosphoribosyltransferase (HGPRT) gene and any immunoglobulin-producing cells. The absence of HGPRT and culturing in specific growth media inhibits de novo synthesis of nucleic acids allows for positive selection of cells that receive selective resistance by fusion with the primary B-lymphocytes or hybridoma cells.

Phage display was developed in 1985 by George P. Smith and Gregory P. Winter and was the subject of the 2018 Nobel Prize in Chemistry.⁶⁰ This approach clones the variable heavy (VH) and variable light (VL) segments from isolated human B-lymphocytes with the filamentous vector of a bacteriophage. This bacteriophage is then used to infect *E. coli*, which then causes small segments of VH and VL segments (the active regions of an antibody) expressed on the cell surface of each *E. coli*. These cells can then be exposed to an antigen and evaluated for binding *in vitro*. Cells that bind are then selected, isolated, and expanded. Plasmids from those *E. coli* are purified and sequenced to determine the specific VH and VL segments. Variations on this original method have also been developed in other species, such as yeast.⁶¹

Although both techniques are major innovations in immunology and have laid the foundations for immune therapy, each has their pros and cons in their use in humans. The traditional hybridoma approach makes monoclonal antibodies that have the Fc region of a mouse, which will cause immunogenicity when used as therapy in humans. This can be overcome by either creating a fragment of an antibody (Fab) or utilizing a patented transgenic mouse that expresses human antibodies. In addition, mouse monoclonal antibodies can have the Fc region swapped for a human Fc region, creating a chimeric antibody. Phage display approaches allow for enrichment with

higher affinity in an unbiased and more efficient approach. These antibodies can easily be modified to express the normalized human heavy chain, reducing immunogenicity seen in mouse monoclonal antibodies. However, the phage display system is problematic as the sequences of proteins themselves are not full antibodies and a secondary cloning and expansion in mammalian cells is necessary. Lastly, phage display binding is based on *in vitro* binding, which may cause significant false positives.

3.3. Overview of screening strategy

Our approach to screening antibodies is focused on two main objectives: 1) identification of PLXDC1 and 2) receptor activation and endothelial cell killing. This is clinically focused with the intention to identify patient populations that would benefit from PLXDC1-targeted therapy and produce a therapeutically active biologic. As each antibody can specifically target and identify unique tertiary and quaternary protein structures, we evaluated each monoclonal antibody across all assays. In a tiered approach, we first screened antibodies that can identify the purified PLXDC1 protein by ELISA or western blot. We then confirmed their ability to bind PLXDC1 in either heterologous expression systems (e.g. HEK293T cells) or endogenous PLXDC1 (e.g. human tissue samples). We determined their ability to activate receptors by measuring downstream transcriptional events specific to the receptor. Afterwards, we evaluated them across *in vitro* and *ex vivo* endothelial cell assays known to have an intact cell killing pathway that is specific to PLXDC1 activation. We performed proof of concept experiments with mouse monoclonal antibodies and then began development of human antibodies.

Ultimately, each antibody with functional activity *in vitro* must be appraised *in vivo*. To accomplish this, we developed a knock-in transgenic mouse that expressed the human PLXDC1 protein and a knockout mouse to demonstrate the specificity of PLXDC1 activation. *In vivo* assays of neovascularization, specifically oxygen-induced retinopathy, laser-induced neovascularization, and skin-grafted tumors, will be used to confirm therapeutic activity.

3.4. Materials and Methods

The cells, reagents, and equipment used in the experiments described in this chapter are listed in Table 3-1.

3.4.1. Large scale PLXDC1 protein production and purification

To produce a large quantity and highly purified recombinant PLXDC1, we utilized a transient expression system in mammalian HEK293 cells designed for rapid and high-yield expression called Expi293. In short, Expi293 cells are high-transfection efficiency HEK293 cells that survive in serum free conditions, in suspension, and at high density. Expi293 cells were thawed, passaged, and cultured to a density of 7.5×10^7 cells/mL in a sterile 30 mL flask at 37°, 8% CO₂ on an orbital shaker rotating at 125 rpm. Each 30 mL flask approximately produced 1 mg of highly purified Rim tagged PLXDC1. We transiently transfected Expi293 cells with a custom cDNA construct that constitutively expresses (CMV promoter) a secreted form of PLXDC1 with a N-terminal 6xHis-Rim tag. Transfection was performed by mixing 30 µg of plasmid DNA in 1.5 mL of Opti-MEM and ExpiFectamine 293 reagent in 1.5 mL of Opti-MEM I for 5 minutes. Reagent then was placed on the cells. 24 hours after transfection, two proprietary enhancers (Enhancer 1 and Enhancer 2) were added. Four days after transfection, the entire flask was harvested, spun down for 10 minutes

to remove cellular debris/contents. Supernatant was then either used fresh or frozen for later protein purification.

The supernatant protein was purified using affinity chromatography. First, we neutralized the supernatant by adding NaH_2PO_4 to a final concentration 50 mM and 0.5 M NaCl to increase binding efficiency. Supernatant was then run over a column of Nickel NTA agarose, washed with 0.5 M NaCl once and then 10 mM of imidazole in PBS. Purified PLXDC1 was eluted with 5 mL of 150 mM of imidazole. Evaluation of total protein concentration was performed by gel electrophoresis and SYPRO Ruby protein gel stain. Confirmation of PLXDC1 was performed by gel electrophoresis and western-blot analysis utilizing both a custom polyclonal PLXDC1 and Rim monoclonal antibody.

3.4.2. Mouse monoclonal antibody production

Mouse monoclonal production was performed by immunizing C57BL/6 mice with purified PLXDC1 for five immunizations. Blood was obtained prior to immunization and after immunization to compare immunogenicity of the antigen. Serum was isolated from the gross blood by centrifugation. Direct enzyme-linked immunosorbent assay (ELISA) was performed (detailed description later) to determine the antibody titer. Once titer was sufficient, mice were sacrificed with their spleen dissected, disassociated, and fused with mouse melanoma Sp2/0 cells. Fused cells were plated in individual wells of a 96 well dish. Cells are grown and passaged and supernatant collected for binding and activity assays (described below).

3.4.3. Large scale human library antibody screening

A human antibody library utilizing the display methodology of over 100 billion antibodies was exposed to purified PLXDC1. Binding to purified PLXDC1 indicated high affinity efficiency. Further enrichment for binding efficiency was assessed by comparing activated receptor versus non-activated receptor. Binding efficiency was compared by ELISA titers and calculated by dividing the activated receptor titer by the full-length receptor titer. Differential binding of greater than 1.5 or less than 0.5 were selected for further study.

3.4.4. Antibody binding assays

To validate antibody binding to protein, enzyme-linked immunosorbent assay (ELISA), western blot, immunocytochemistry, and immunohistochemistry were performed.

ELISA

Utilizing the aforementioned purified PLXDC1 protein, we coated a 96-well dish with PLXDC1 protein in 50 mM of Na₂CO₃-NaHCO₃ at 2 µg/mL at 100 µL / well at 4° Celsius overnight. Plates were then blocked with 200 µL / well of Casein at room temperature for at least 1 hour. Monoclonal antibody clones were diluted into 1% BSA/PBS and incubated overnight at 4° Celsius. Wells were then washed with PBS three times and then incubated with HRP-labeled anti-IgG at a dilution of 1:5000 at 37° for 1 hour. Substrate solution was 100 µL of TMB per well at RT for 30 mins and OD reading was performed on a POLARStar OMEGA plate reader at 450 nm.

Western Blot

Western blot was performed utilizing 1 µg of antigen per lane. Gel electrophoresis was performed on a 12% SDS-PAGE gel and transferred onto a nitrocellulose membrane. Supernatant from each hybridoma clone was used as primary antibody. Secondary antibody was an HRP-Goat Anti-Mouse IgG (Fc) at a 1:10,000 dilution.

Immunocytochemistry

Immunocytochemistry (ICC) was performed on both HEK293T and COS-1 cells. Both cells were transiently transfected with His-Rim tagged PLXDC1. We performed both live- and permeabilized-cell staining. These procedures differ where incubation of primary antibody occurs prior to fixation and permeabilization in live cell-staining or cells are fixed and permeabilized prior to primary antibody incubation in permeabilized-cell staining. After 48 hours, primary dilution ratio was 1:100 with the supernatant of each hybridoma clone, 1:100 with monoclonal PLXDC1 antibody, or 1:100 with monoclonal anti-RIM antibody for 1 hour at 37° Celsius. Cells were fixed with 4% paraformaldehyde or methanol at 4° for 15 or 60 minutes, respectively. Cells were then washed with PBS three times, blocked and permeabilized with 5% normal goat serum with 0.5% of Triton X-100 for 1 hour at room temperature if permeabilized-cell staining was performed. Cells are incubated in DAPI (1:1000), secondary AlexaFluor 594 anti-Rabbit IgG, and AlexaFluor 488 anti-Mouse IgG at 1:1000 dilution suspended in the aforementioned blocking solution for 1 hour at room temperature. Co-staining of Rim and PLXDC1 was evaluated with fluorescent microscopy.

Immunohistochemistry

Immunohistochemistry (IHC) was performed on human tumors. Human tumors were freshly acquired from UCLA Translational Pathology Core Laboratory (TPCL). Tissues were fresh frozen by placing them directly into Optimal Cutting Temperature (OCT) compound and then freezing them in the vapors of liquid nitrogen. Tissues were cut to 10-micron sections and fixed with methanol, blocked and permeabilized with 5% normal goat serum/0.5% Triton X-100/PBS. Monoclonal antibody dilution was 1:200 and secondary antibody was a conjugated HRP anti-mouse IgG at 1:1000. DAB (3, 3-diaminobenzidine) was used as a substrate and staining is confirmed by light microscopy.

3.4.5. *In vitro* assays of receptor activation

3.4.5.1. Cell receptor activation assay

Receptor activation is as previously detailed in Chapter 2.5.4.1. Rather than a small molecule PLXDC1 agonist, monoclonal mouse antibody or human Fab was utilized at 200 nM final concentration.

3.4.5.2. Cell adhesion assay

To determine the antibodies ability to inhibit normal cell adhesion, immortalized murine endothelial cells were trypsinized and resuspended in serum free media with monoclonal antibodies at 500 nM or 1000 nM. Four hours later, cells were evaluated under light microscopy to determine their ability to adhere the plastic well. Twenty-four hours after resuspension, cell viability was determined by MTT assay (previously discussed) or co-staining with fluorescein diacetate and propidium iodide.

3.4.5.3. Endothelial cell death assay

Endothelial cell death assay as previously discussed in 2.5.4.3. Rather than a small molecule PLXDC1 agonist, monoclonal mouse antibody or human Fab was utilized at 500 nM final concentration.

3.4.6. *Ex vivo* 3D endothelial cell culture

To determine whether each antibody can effectively kill pathogenic blood vessels, we developed an *ex vivo* 3D endothelial cell culture. Tumors are isolated freshly from human patient or mice tumors. Tumors were sectioned into approximately 1 mm x 1 mm cubes and placed into Matrigel, a solubilized basement membrane isolated from Engelbreth-Holm-Swarm (EHS) mouse sarcomas, on a 48-well or 24-well dish. Growth factor enriched medium was then added to each well and changed every 3-4 days. Endothelial cells grow and become visible within 3-7 days, depending on tumor type.

To screen each antibody, monoclonal antibodies or Fabs were added to the media at 500 nM final concentration. Endothelial cells were monitored for up to 1 week to determine whether morphological changes, suggesting cell death, are present. To confirm cell viability, fluorescein diacetate and propidium iodide were added to visualize alive and dead cells, respectively.

3.4.6.1. Lentivirus transfection of 3D endothelial cell culture

PLXDC1 lentivirus was utilized to ectopically express human PLXDC1 in 3D endothelial cell cultures to determine efficacy and specificity of monoclonal antibodies. Specifically, human PLXDC1 was cloned into a lentiviral vector with constitutively active promoter (CMV). Lentiviral

plasmid was co-expressed with helper plasmids (PLP1, PLP2, and PMD2.G) and GFP lentivirus at a 5:1 ratio in HEK293T cells in serum-free medium. 48-hours later, supernatant was harvested, ultra-centrifuged at 140,000 rpm for 1 hour. Virus was resuspended in SFM and then applied to the 3D endothelial cell culture with 8 µg/mL of polybrene. Media were changed to growth factor enriched media 24 hours after transduction. Fluorescence was noted approximately 3-4 days after viral transduction.

3.4.7. *In vivo* endothelial cell models

3.4.7.1. Humanized transgenic mouse model

To evaluate the efficacy of human specific PLXDC1 monoclonal antibodies in killing endothelial cells, we developed a knock-in mouse model utilizing homologous recombination. Briefly, the construct is the human PLXDC1 coding sequence with reporter fluorescent protein in between two homology arms that flank mouse exon 1 of *Plxdc1* (Figure 3-1). In addition, a floxed neomycin cassette and diphtheria toxin are present for positive and negative selection of embryonic stem cells, respectively. This construct was linearized and then injected into mouse embryonic stem cells. Embryonic stem (ES) cells are plated on mouse embryonic fibroblast (MEF) feeder cells (from neomycin resistant strain) treated with mitomycin C to prevent proliferation. In the presence of leukemia inhibitory factor (LIF), ES cells are plated and G418 selection is added (200 µg/mL). After 2-5 days of G418 selection, individual ES cells are picked and plated into a 96 well dish already coated with MEF cells. Selected ES cells are grown and genomic DNA is isolated in a subset to determine correct knock-in construct. Transgene is confirmed by first by PCR at both the 5' and 3' end of the knock-in construct. Those that are positive are then secondarily confirmed with real-time PCR to determine if single copy integration occurs. Positive ES cells are then expanded

and introduced into an accepting mother. After the mom gives birth, chimeric mice are then confirmed and evaluated for germ-line transmission for the F1 generation. Mice are then cross-bred for a homozygous knock-in.

3.4.8. Laser induced choroidal neovascularization (CNV) and intravitreal injections.

To evaluate the effect of *in vivo* endothelial cell death, we performed laser induced choroidal neovascularization.⁶² Mice were anesthetized and eyes were dilated with tropicamide and phenylephrine. Laser settings were 532 nm wavelength, 50-micron spot sizes, pulse duration of 70 ms and 250 mW power. Laser spots are placed circumferentially around the optic nerve. Approximately 5-8 lesions were performed per mice eye. Prior to awakening, mice eyes were disinfected with betadine. A small incision with a 30-gauge insulin syringe was made approximately 1 mm behind the limbus. Then a 33-gauge Hamilton syringe filled with 1 μ L of concentrated antibody was inserted into the incision, with careful attention to avoid affecting the lens. The 1 μ L of antibody was then slowly pushed into the vitreal cavity. After injection, eyes were then lubricated with antibiotic ointment and mice were recovered on a heated pad. Seven days after laser-induced CNV and intravitreal injections, mice were sacrificed and eyes were enucleated.

Lectin staining was performed to stain the pathogenic choroidal neovascularization. After eye enucleation, the cornea and lens were micro-dissected out. Eyes were then fixed in 4% paraformaldehyde for 45-60 mins at room temperature, washed three times, and placed in blocking media (5% goat serum 0.5% Triton X-100) for 45-60 mins at room temperature. Eye cups were

incubated in lectin at 1:500 for 3 hours at room temperature and washed. Four relaxing cuts are made and eyes are mounted for evaluation with a fluorescent microscope.

3.5. Results

3.5.1. Novel mouse monoclonal antibodies bind and identify recombinant and endogenous PLXDC1

We screened 96-isolated hybridoma and identified 3 monoclonal antibodies that can reliably detect PLXDC1 and 8 monoclonal antibodies that can kill endothelial cells *ex vivo*.

First, we produced highly concentrated purified PLXDC1 through affinity purification. Figure 3-2 shows a western blot probed with anti-human PLXDC1 polyclonal antibody. PLXDC1 was identified in high concentration in the elutions (total 1 mg per 30 mL of resuspended HEK293T cells). This purified protein was then used as the immunizing antigen for the production of mouse monoclonal antibodies.

ELISA, western blot, immunocytochemistry and immunohistochemistry, confirmed Mouse monoclonal antibody binding. The ELISA readings of 96 different monoclonal antibody supernatants is shown in Figure 3-3 with the positive and negative control in the lower right-hand corner. High affinity clones were then selected for large-scale monoclonal production. Western blot analysis confirmed detection by mouse monoclonal antibodies against recombinant PLXDC1 antigen (Figure 3-4). Mouse monoclonal antibodies appear to mostly identify the PLXDC1 dimer. However, some monoclonal antibodies (right) demonstrate identification of either the monomeric or a degraded form of the PLXDC1 protein. To determine whether monoclonal antibodies could

recognize PLXDC1 in native confirmations, we ectopically expressed PLXDC1 in HEK293T (Figure 3-5) and COS-1 cells. We performed live cell staining, which demonstrated red fluorescence in a membrane pattern, confirming the ability of the monoclonal antibody to detect the receptor. This co-localized with rim tag (not shown). Furthermore, we evaluated the monoclonal antibody's ability to detect PLXDC1 in human fresh frozen cancer tissues. The monoclonal PLXDC1 antibody shows staining in an endothelial pattern in a hepatocellular carcinoma. Staining pattern is consistent with VEGFR2, another known endothelial specific angiogenic receptor that acted as a positive control (Figure 3-6).

3.5.2. Novel mouse monoclonal antibodies activate PLXDC1 and cause endothelial cell death

Endothelial cell killing was confirmed by 3D endothelial cell culture. In the presence of monoclonal antibodies that target PLXDC1, significant endothelial cell death was noted in human liver, pancreas, renal cell cancer endothelial cell cultures. Propidium iodide (red) and fluorescein diacetate (green) was utilized to demonstrate dead and alive cells, respectively. At day 4 endothelial cells exhibit no signs of cell death. However, 6 days of incubating in 200 nM of monoclonal antibody, significant endothelial cell death is noted (Figure 3-7). Interestingly one monoclonal antibody showed cross-reactivity in endothelial cell culture grown from mouse lung cancer (Figure 3-8).

The mouse monoclonal antibody was proof-of-principle that a monoclonal antibody targeted against PLXDC1 can bind and activate PLXDC1. Activation of PLXDC1 in endothelial cells can then cause cell death and potentially act as a potential anti-angiogenic therapy.

3.5.3. Human Fab library screen yielded highly enriched antibodies that preferentially bind the activated PLXDC1

We screened 200 billion human Fab clones and performed serial selections to identify 100,000 high affinity clones. From these clones, we selected 100 clones that could preferentially bind the activated form of PLXDC1. Out of the 100 screen antibodies, 30 were further developed for functional activity.

100-screened clones were exposed and evaluated for their ability to bind recombinant PLXDC1. Production of these Fabs was confirmed by SDS-Page (Figure 3-9). To determine whether there was selective binding to activated PLXDC1 receptor, ELISA was performed comparing the activated or full-length receptor. An example of 96 different clones that were assessed by differential ELISA is shown in Figure 3-10. The red highlight boxes indicate clones that bound to PLXDC1 with high affinity. In addition, clones with a highly differential (either greater than 1.5 or less than 0.5) ratio between activated and full-length receptor were selected for further analysis. As human Fab do not have a heavy chain, we could not perform any staining experiments (immunohistochemistry or immunocytochemistry)

3.5.4. Human Fabs inhibit endothelial cell adhesion and cause secondary endothelial cell death

We confirmed that the humanized Fab was able to bind and inhibit endothelial cells from adhering. We resuspended endothelial cells with 500 nM of Fab and evaluated at 4 hours and 24 hours to determine the extent of adhesion. On light microscopy, cells appear to remain in a "balled-up"

morphology and were unable to adhere the plastic, which can be seen in the control Fab or no Fab added condition. To confirm that these cells undergo cell death, we performed a propidium iodide and fluorescein diacetate treatment (Figure 3-11). Cells that do not adhere then undergo apoptosis. Interestingly, no difference between wild-type and transgenic mouse endothelial cells was noted (data not shown).

3.5.5. Human Fabs cause endothelial cell death in *ex vivo* 3D endothelial cell culture

Ex vivo endothelial cell cultures were utilized to determine whether humanized Fab were able to identify and kill endothelial cells in a condition that mimics endothelial cells in vivo. Human tumors were freshly embedded into a matrix that contained basement membrane and growth factors. Endothelial cells were grown for 1-2 weeks. Fab at 200 nM that was initially added showed no endothelial cell death. We then co-transduced endothelial cells with PLXDC1 and EGFP virus and evaluated endothelial cell loss over one week. Addition of Fab at 500 nM showed significant reduction of EGFP, suggesting endothelial cell death secondary to the humanized Fab (Figure 3-12).

3.5.6. Human Fabs cause partial inhibition of CNV in a laser-induced retinopathy model

We evaluated human Fab efficacy in laser-induced CNV. Concentration of Fab was dependent on the concentration of the humanized Fab, ranging from 1-15 μ M. Mice retinas were lasered and subsequently injected with human Fab or PBS. Seven days later, mice were sacrificed and retinas were enucleated and stained with lectin to evaluate degree of CNV inhibition (Figure 3-13). Compared to PBS, antibody 42 and 113 showed signs of CNV inhibition while antibody 46 showed no CNV inhibition, with similar size as control.

3.6. Discussion

We developed monoclonal antibodies utilizing both common antibody production methods: traditional hybridoma and modern phage display. We provide evidence that mouse monoclonal antibodies can detect PLXDC1 expression in simplified (*in vitro* heterologous expression systems) and complex (*in vivo* immunohistochemistry of human sections) conditions. Furthermore, we created antibodies that had functional activity *in vitro*, *ex vivo*, and *in vivo* in killing pathogenic blood vessels. Although significant future studies are necessary to optimize efficacy and potency in human angiogenic diseases, this study suggest the potential for PLXDC1 targeted therapy.

Although monoclonal antibody production is normally performed through one approach (either hybridoma or phage display), we approached PLXDC1 targeted therapy in a step-wise manner. The hybridoma studies were a proof-of-principle to fuel large-scale evaluation of functional antibodies by phage display. Hybridoma approaches are well characterized and practically less expensive to perform compared to their phage display counterparts, most commonly due to intellectual protections with library phage display systems. However, without access to transgenic mice that express human antibodies, translating mouse monoclonal antibodies into humans requires significant antibody modifications.⁶³ Translation of a mouse monoclonal antibody into a human antibody was also originally pioneered by Sir Greg Winter through complementarity determining region (CDR) grafting.⁶⁴ Furthermore, hybridoma approaches are limited by the mouse immune system, where sub-populations of antibodies are over represented, leading to a less diverse antibody repository. This approach may work well for inactivating antibodies where high affinity is sufficient for therapeutic effect, but antibodies that can enhance receptor activation or functionality can be influenced by many factors, such as the binding epitope, affinity, valency, and

degree of receptor occupancy.⁶⁵ Furthermore, subtle changes in receptor conformations may have significantly different coupled downstream signaling pathways and cellular outcomes.^{66,67} Therefore, utilizing a unbiased screening approach that incorporates a wide variety of antibodies (such as the one performed with phage display in this study), more systematically evaluates therapeutic antibodies that may activate subtle conformational changes that bias the receptor in endothelial cells towards a cell death pathway.

Although no antibody that activates a membrane receptor exists for clinical use, examples of receptor activating antibodies do exist in nature and many groups are currently investigating antibody-mediated activation as a possible therapeutic approach.⁶⁵ Most importantly, *in vitro* efficacy does not ensure *in vivo* efficacy. The most notable example is Grave's disease, where autoantibodies directed against the thyrotropin receptor (TSHR) cause autonomous production of thyroid hormones. Interestingly, these antibodies are monoclonal, low in concentration in the human serum, typically within the nanogram per milliliter range, and less frequent than polyclonal autoantibodies towards thyroid peroxidase.⁶⁸ In fact, the majority, but not all, of monoclonal antibodies produced by immunizing with purified proteins or peptides approach fail to recapitulate Grave's disease.⁶⁹ To overcome this, groups have co-expressed the TSHR with MHC class II molecules⁷⁰, immunized directly with the cDNA⁷¹, or ectopically expressed TSHR through adenovirus.⁷² This suggest that the native confirmation of the receptor with post-processing *in vivo* may be necessary to develop antibodies with targeted activation. Chazenbalk et al. suggest that the portion of the antibody that binds the free A subunit and not the TSH holoreceptor may actually initiate or amplify the autoimmune response to TSHR.⁶⁸ This may be one of explanation for the incomplete efficacy *in vivo* seen in this study, as PLXDC1 is expected to be expressed in

pathogenic angiogenesis. In addition, human Fabs were targeted against human PLXDC1; therefore, efficacy seen in mice may be incomplete as the human and mouse, although highly conserved, are different. Regardless, findings in our study provide evidence for PLXDC1-targeted therapy but further studies *in vivo* are necessary to confirm and optimize efficacy.

In conclusion, this thesis provides evidence that monoclonal antibodies against PLXDC1 can detect and activate PLXDC1 *in vitro* and *in vivo*. This activation prevents normal cellular adhesion through ITGB1 and anoikis. Anti-mediated PLXDC1 activation may be a potential therapeutic alternative in targeting anti-angiogenesis.

Table 3-1 List of cell lines, reagents, and equipment

	Material/ Equipment	Description	Manufacturer
Cell Lines	COS-1 Cell	Monkey kidney fibroblast cells	ATCC
	HEK293T Cell	Human embryo kidney 293 cell transformed with T-antigen	ATCC
	Expi293™ Cells	Expi293™ Cells	ThermoFisher Scientific
Reagents	Alexa Fluor 488 dye Rabbit IgG	Alex Fluor 488-conjugated Rabbit IgG antibody	ThermoFisher Scientific
	Alex Fluor 594 Mouse IgG	Alex Fluor 594-conjugated Mouse IgG antibody	ThermoFisher Scientific
	Casein	Casein Protein Blocking Reagent	ThermoFisher Scientific
	DAB	3,3 – diaminobenzidine HRP substrate	Vector Labs
	DMEM	Dulbecco's Modified Eagles Medium	Corning, Mediatec, Inc.
	DMSO	Dimethyl sulfoxide	Corning, Mediatec, Inc.
	Doxycycline	n/a	Sigma
	Dylight 680 Ab	Dylight 680-conjugated goat anti-mouse antibody	Pierce, Thermo
	Expi293™ Expression System Kit	Contains transfection reagent and enhancers for transient transfection of Expi293™ Cells	ThermoFisher Scientific
	FBS	Fetal Bovine Serum	Corning, Mediatec, Inc.
	HBSS	Hank's Balanced Salt Solution	Hyclone, GE Healthcare Life Sciences
	HRP-Goat, Anti-Mouse IgG (Fc)	Anti-Mouse IgG conjugated with horse radish peroxidase	Sigma, Cat #: A-0168
	IRDye 800CW Ab	IRDye 800-conjugated goat anti-rabbit antibody	Li-Cor
	Normal Goat Serum	Blocking reagent	SouthernBiotech
	jetPRIME	DNA transfection reagent	Polyplus-transfection
	Lectin	Fluorescently labelling of endothelial cells	
	Luciferase assay system	Lysis buffer, lysis reagent	Promega
	Methanol	Methanol	FisherScientific
	monoclonal α -Rim	Monoclonal anti-Rim antibody	n/a

	MTT reagent	n/a	Life Science Research Products
	Optimal Cutting Temperature (OCT)	Embedding reagent for tissue sectioning	FisherScientific
	Paraformaldehyde	Fixative Reagent	FisherScientific
	PBS	Phosphate Buffered Saline	Corning, Mediatec, Inc.
	Phenol red free DMEM	Dulbecco's Modified Eagles Medium	Corning, Mediatec, Inc.
	Phenylephrine 2.5%	Alpha-1 adrenergic receptor agonist, dilating eye drop	Akorn Pharmaceuticals, Inc.
	Polybrene	Transfection Reagent	EMD Millipore, Inc.
	Polyclonal α -HA	Polyclonal anti-HA antibody	Genemed Synthesis
	SYPRO Ruby Protein Gel Stain	Permanent protein stain	Molecular Probes
	Triton X-100	Triton X-100 surfactant	Omnipur, Millipore
	Tropicamide 1.0%	Muscarinic receptor m4 inhibitor, dilating eye drop	Akorn Pharmaceuticals, Inc.
	Trypsin	0.05% trypsin	Corning, Mediatec, Inc.
	Trypsin Inhibitor	DTI, defined trypsin inhibitor	Gibco, Life Technology
Equipment	96-well plate	96-well, flat and clear bottom	Genesee Scientific
	33-gauge Hamilton Syringe	Syringe	Hamilton Company
	31-gauge insulin syringe	Insulin Syringe	Becton Dickinson Company
	Fluorometer	Fluorometer	Horiba Jobin Yvon, Inc.
	POLARstar Omega	n/a	BMG Labtech
	Micron IV	Retinal imaging and laser apparatus	Phoenix Technology Group

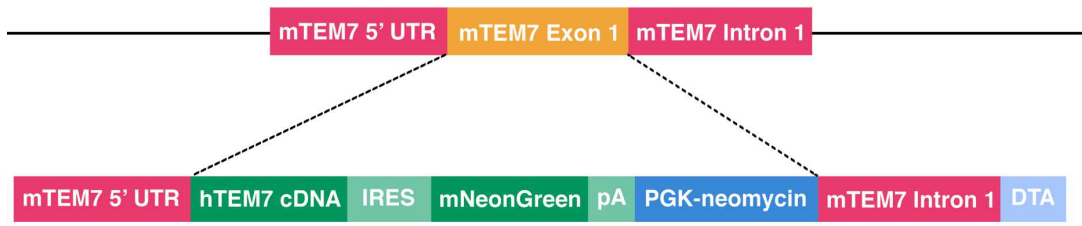


Figure 3-1. Genomic engineering strategy for knock-in PLXDC1 (TEM7) transgenic mouse

Construct developed for knock-in human PLXDC1 (TEM7) mouse model where mouse exon 1 is replaced with the human PLXDC1 (TEM7) cDNA. A reporter fluorescent protein and positive and negative selection criteria are present.

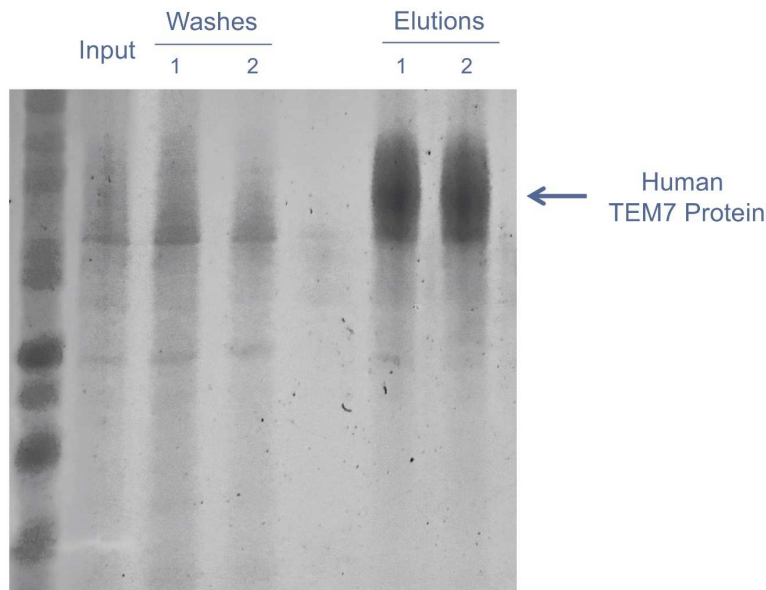


Figure 3-2. Purification of PLXDC1 (TEM7)

Western blot analysis showing production of highly purified and concentrated human PLXDC1 (human TEM7) protein. This purified protein preparation was utilized as the antigen for monoclonal antibody immunization.

Clone NO.	1A2	1A10	1A11	1D8	1D10	1D11	1E6	1H11	2A5	2A7
Antigen1OD	1.614	0.631	1.812	1.592	0.224	1.702	0.672	0.665	1.726	0.311
Antigen2OD	1.609	0.326	1.707	1.394	0.135	1.449	0.222	0.733	0.308	0.222
Clone NO.	2B3	2B4	2B5	2B8	2B12	2C3	2D6	2E7	2F4	2F6
Antigen1OD	1.883	0.593	1.938	1.126	0.435	1.889	0.154	1.732	1.747	0.717
Antigen2OD	1.621	0.286	7.875	0.583	0.212	1.360	0.066	1.546	1.616	0.535
Clone NO.	2G9	2H1	2H2	2H7	2H8	2H9	3A1	3A6	3B5	3B6
Antigen1OD	0.320	0.229	1.517	0.235	0.222	1.715	1.808	0.170	0.141	1.808
Antigen2OD	0.095	0.116	1.239	0.059	0.150	1.673	1.833	0.120	0.152	1.814
Clone NO.	3D8	3D12	3E2	3E3	3G5	3G6	3H12	4A2	4A3	4C4
Antigen1OD	1.659	0.286	0.168	1.711	0.332	1.895	1.705	0.196	1.868	0.310
Antigen2OD	1.112	0.443	0.226	1.592	0.144	1.527	1.815	0.133	1.950	0.417
Clone NO.	4C8	4D8	4D9	4D10	4E6	4E10	4F5	4G6	4G10	4G11
Antigen1OD	0.856	1.595	0.716	1.764	0.251	1.983	0.936	1.733	1.431	1.779
Antigen2OD	1.005	1.555	0.622	1.540	0.230	1.440	0.610	1.944	1.449	1.894
Clone NO.	4H3	4H5	5A7	5C4	5D1	5D2	5D3	5E4	5E5	5F12
Antigen1OD	0.920	1.513	0.107	1.830	0.422	0.437	0.283	0.152	0.934	0.721
Antigen2OD	0.113	1.634	0.069	1.825	0.201	0.131	0.376	0.165	0.687	0.334
Clone NO.	5G2	6C1	6C2	6C10	6E3	6G1	6G8	6G9	6H1	7B1
Antigen1OD	1.537	0.089	1.732	1.583	0.592	1.821	0.128	1.885	1.847	2.011
Antigen2OD	1.253	0.074	1.307	1.687	0.518	1.621	0.198	1.760	1.963	0.450
Clone NO.	7B3	7C4	7C12	7D4	7D5	7D6	7F7	7G5	7G6	7H1
Antigen1OD	0.348	0.242	1.690	0.359	2.015	1.831	1.841	0.441	2.007	0.118
Antigen2OD	0.135	0.175	1.722	0.12	1.613	1.682	1.603	0.115	1.775	0.057
Clone NO.	7H2	7H6	8A1	8A6	8B1	8B7	8B12	8C5	8D1	8D9
Antigen1OD	1.497	0.144	1.734	1.605	0.140	1.176	0.131	0.090	1.822	1.746
Antigen2OD	0.447	0.133	1.502	0.670	0.110	1.160	0.103	0.080	1.636	1.599
Clone NO.	8E4	8F5	8G12	8H10	8E3	8F4			POS	NEG
Antigen1OD	0.545	1.691	0.313	1.862	1.848	0.484			2.033	0.098
Antigen2OD	0.464	1.771	0.299	1.711	1.195	0.330			2.014	0.098

Figure 3-3. Example of ELISA from hybridoma mouse monoclonal antibody

ELISA performed in duplicate of 96 monoclonal antibody supernatant against PLXDC1 antigen. Note the increased ELISA titers for many antibodies compared to the positive and negative controls (bottom right).

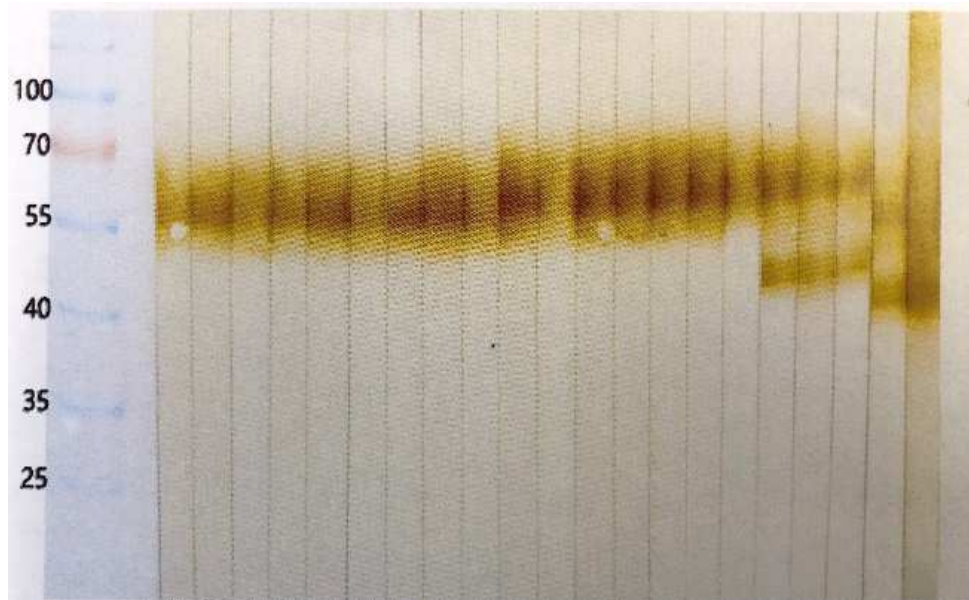


Figure 3-4. Western blot confirms recognition of recombinant PLXDC1 protein by monoclonal mouse antibodies

Western blot analysis of individual hybridoma supernatants of each mouse monoclonal antibody demonstrates recognition of the recombinant immunizing PLXDC1 protein. Interestingly the majority of the antibodies identified the homodimer of PLXDC1 while some (right) show identification of a degraded PLXDC1 or the dimer and oligomer of PLXDC1.

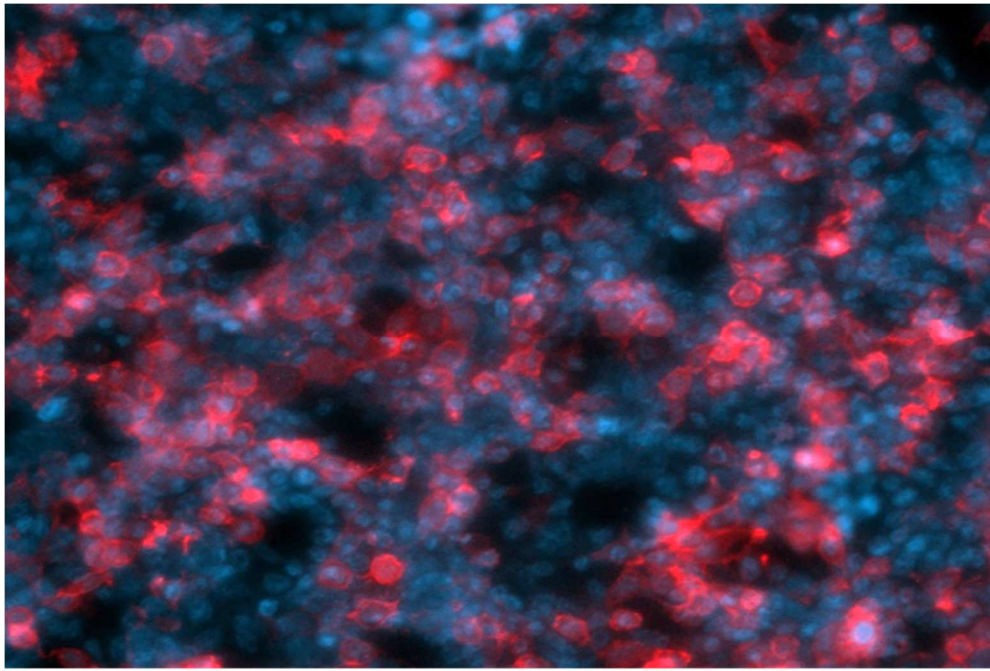


Figure 3-5. Live cell staining of HEK293 ectopically expressing PLXDC1

Red fluorescence confirms one mouse monoclonal antibody's ability to bind PLXDC1 in the native confirmation. DAPI counter stains confirms that the staining is membrane bound and cytosolic.

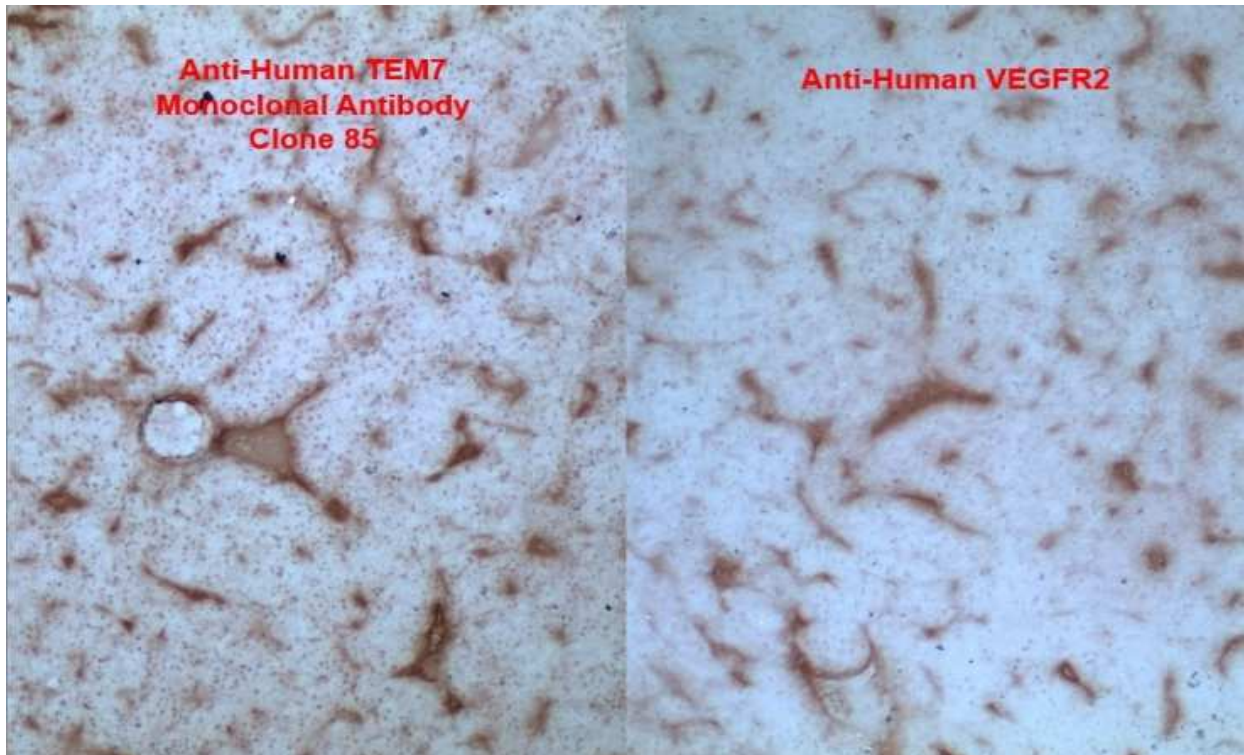


Figure 3-6. Immunohistochemistry with anti-human PLXDC1 (TEM7) mouse monoclonal antibody

Fresh frozen and fixed human hepatocellular (liver) cancer shows staining of the microvasculature more prominently by the monoclonal antibody against PLXDC1 (TEM7) (left) as compared to a polyclonal antibody against human VEGFR2 (right).

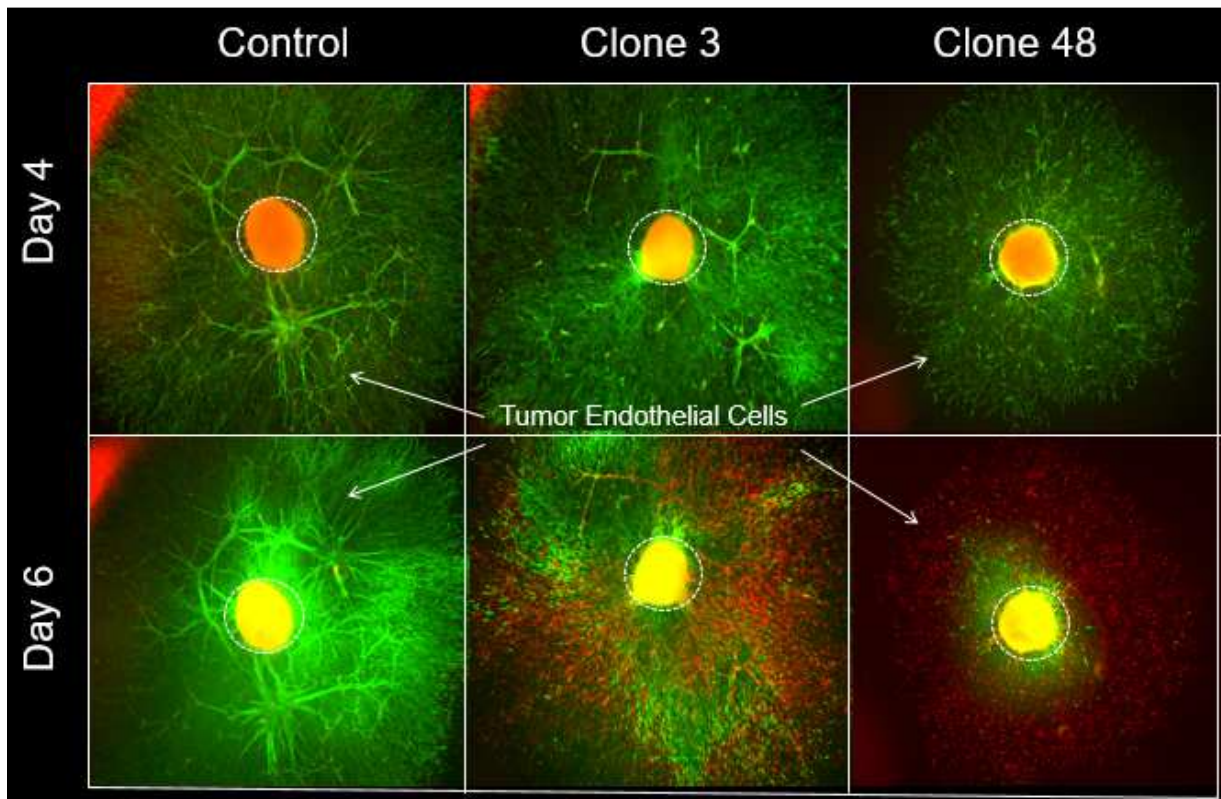


Figure 3-7. Mouse monoclonal antibody causes endothelial cell death in human *ex vivo* 3D endothelial cell culture

Endothelial cell killing was significantly greater by two monoclonal antibodies compared to control in tumor endothelial organoid culture of human hepatocellular carcinoma. The red signal (propidium iodide) indicates cell death while the green (fluorescein diacetate) signal reflects alive cells.

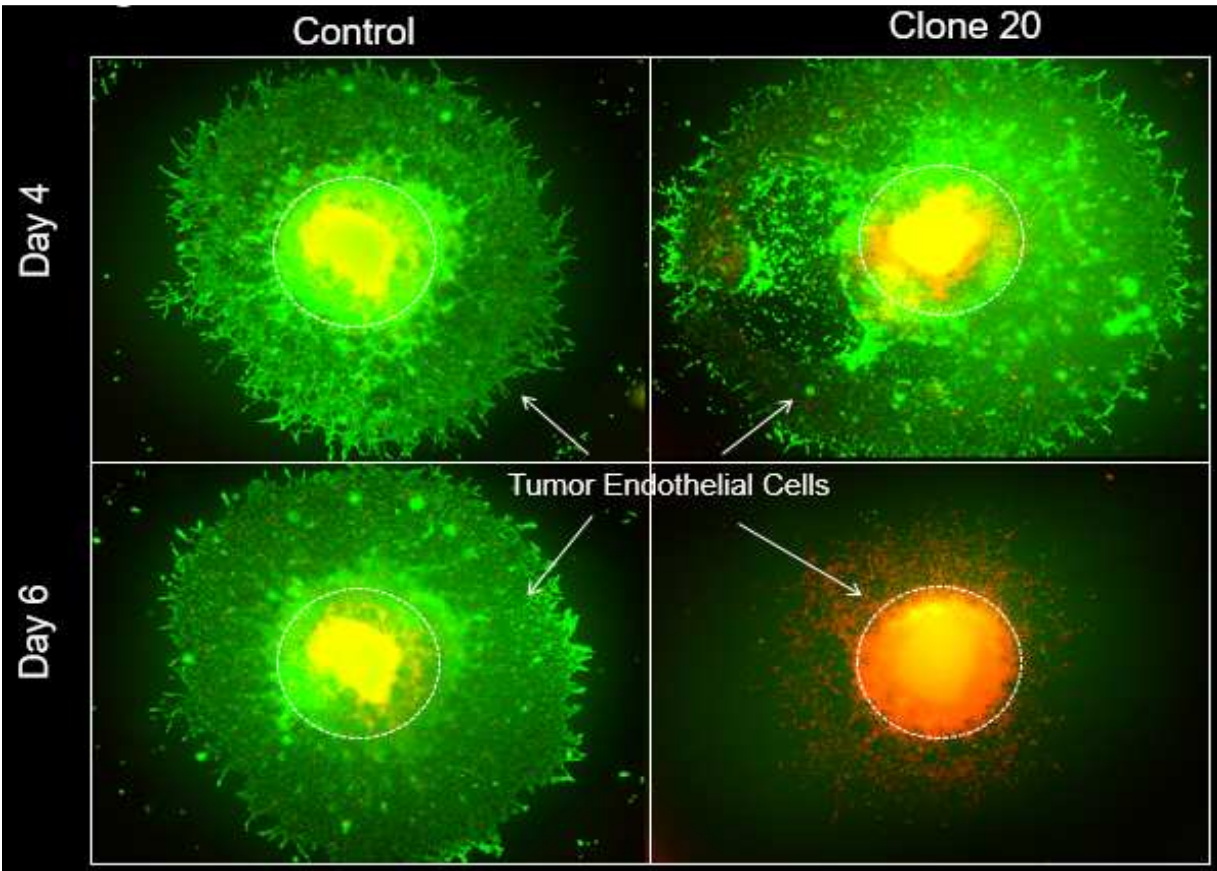
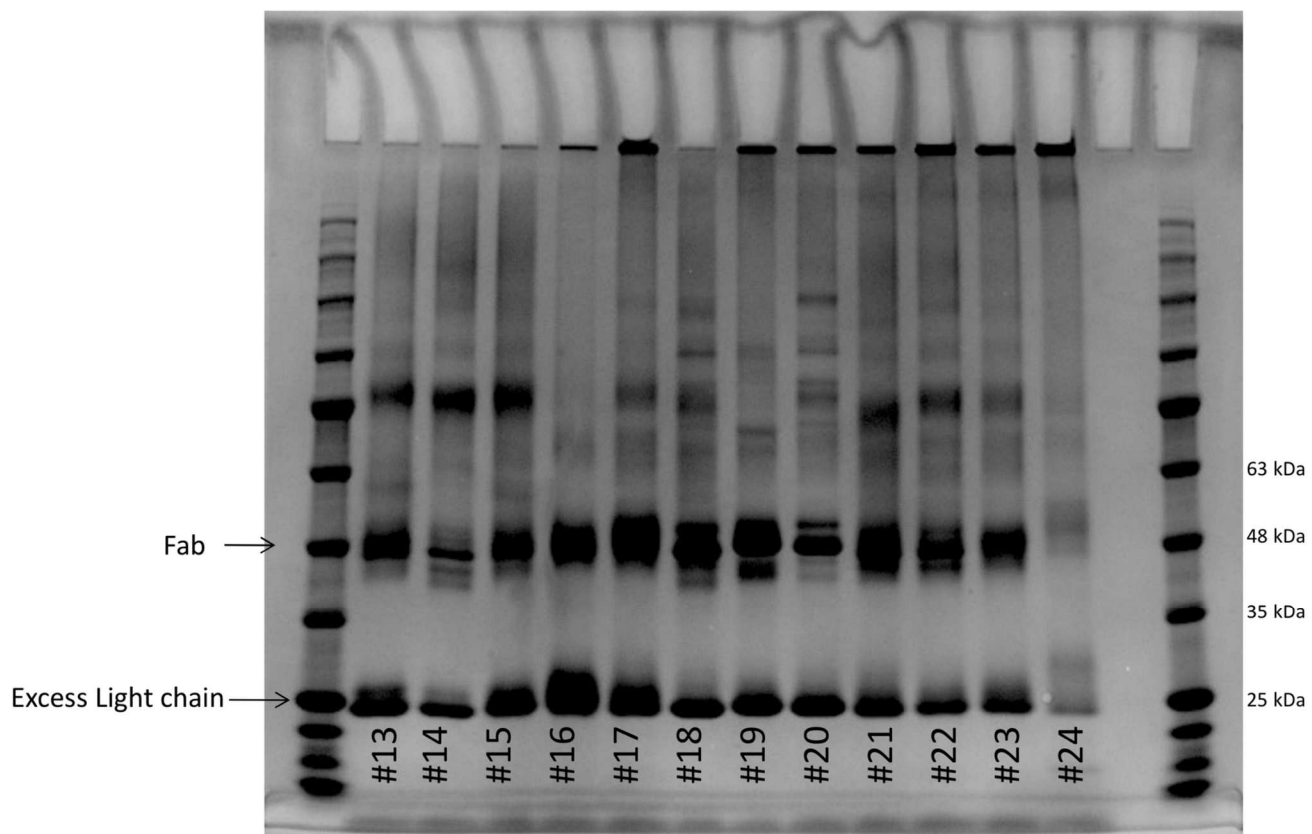


Figure 3-8. Mouse monoclonal antibody causes endothelial cell death in mouse *ex vivo* 3D endothelial cell culture

Endothelial cell killing tumor endothelial cells derived from a mouse colon cancer. One monoclonal antibody showed cross-reactivity with the mouse PLXDC1. The red signal (propidium iodide) indicates cell death while the green (fluorescein diacetate) signal reflects alive cells.



Loaded 3 ug of sample per well

Figure 3-9. SDS-Page show presence of purified Fabs

SDS-Page indicates that the phage display approach was successful in producing purified Fabs.

UCLA-Combined-#5												
2Llbs+RA-S4-P2		2Llbs-No-RA-S4-P2		UCLA-Ag-3Llbs-No-RA-S4-P2								
1	2	3	4	5	6	7	8	9	10	11	12	
A	A4	F1	D1	F10	No-Fab	B1	C3	D1	E4	F5	G5	H6
B	A9	H9	D9	G1	A2	B2	C4	D2	E5	F6	G7	H7
C	B1	H11	D11	G2	A5	B3	C5	D4	E7	F7	G8	H8
D	B7	CTL-Fab#1	E1	G3	A6	B4	C7	D5	E9	F9	G10	H9
E	B9	A5	E2	G4	A9	B5	C9	D9	E10	F12	G11	H10
F	B11	B6	E12	H3	A10	B11	C10	D11	E11	G1	G12	H11
G	C12	B9	F2	H6	A11	B12	C11	D12	E12	G2	H1	CTL-Fab#2
H	E8	B12	F6	H7	A12	C1	C12	E1	F3	G4	H5	No-Fab

UCLA-Combined-#5												
2Llbs+RA-S4-P2		2Llbs-No-RA-S4-P2		UCLA-Ag-3Llbs-No-RA-S4-P2								
1	2	3	4	5	6	7	8	9	10	11	12	
A	0.0946	1.5862	0.7323	4	0.0445	0.2751	0.3553	0.477	0.312	0.876	0.7535	0.3355
B	0.262	0.0451	0.071	0.1333	0.1472	0.2117	0.2672	0.0643	0.7205	0.2261	0.914	1.3487
C	4	0.0423	0.0989	0.0531	0.1842	0.3699	0.2364	0.2799	0.3322	0.4272	0.167	1.4806
D	0.0847	0.0463	0.0971	0.119	0.1492	0.8626	0.2221	0.2468	0.7771	0.3499	0.4972	0.1912
E	0.304	1.4224	0.7777	0.193	0.146	0.3494	0.2879	0.277	0.2279	0.1062	0.2342	0.3864
F	0.1376	0.2912	0.1142	0.1442	0.1108	0.3647	0.1062	0.2845	0.2562	0.1211	0.9216	0.187
G	0.1249	0.3342	0.0975	0.1619	0.2968	0.1225	0.1113	0.1852	0.4762	0.4139	1.4305	0.043
H	0.1066	0.1026	0.1177	0.1044	0.198	0.1699	0.1176	0.1344	0.1412	0.8214	0.1364	0.0467

ELISA-No-RA

UCLA-Combined-#5												
2Llbs+RA-S4-P2		2Llbs-No-RA-S4-P2		UCLA-Ag-3Llbs-No-RA-S4-P2								
1	2	3	4	5	6	7	8	9	10	11	12	
A	0.0995	1.6374	0.722	4	0.0424	0.2868	0.4094	0.4769	0.34	0.8383	0.7922	0.3689
B	0.2909	0.0422	0.0658	0.1479	0.1587	0.2014	0.2459	0.0619	0.7213	0.2021	0.9881	1.3897
C	4	0.0424	0.0871	0.0526	0.1676	0.363	0.2214	0.2167	0.4023	0.4165	0.1698	1.5357
D	0.0851	0.0406	0.0898	0.1062	0.1556	0.8757	0.2075	0.2439	0.7336	0.3427	0.5231	0.1952
E	0.2852	1.743	0.7768	0.1803	0.171	0.3134	0.2716	0.2754	0.2149	0.0994	0.2444	0.4719
F	0.1248	0.2925	0.1138	0.1421	0.1204	0.3348	0.1083	0.2844	0.2539	0.1182	0.9399	0.2091
G	0.1344	0.3211	0.0901	0.1571	0.3459	0.1265	0.1113	0.1832	0.5129	0.3641	1.4241	0.0423
H	0.0859	0.0882	0.1107	0.0907	0.2248	0.1741	0.1047	0.1355	0.155	0.7892	0.1284	0.0468

ELISA+RA

Figure 3-10. ELISA of fab binding affinity between activated and non-activated receptor

An example of the ELISA titers between the activated and non-activated PLXDC1 receptor. Red highlighted indicates high affinity clones. Ratio of activated versus non-activated PLXDC1 receptor of greater than >1.5 or less than <0.5 were selected for further functional screening.

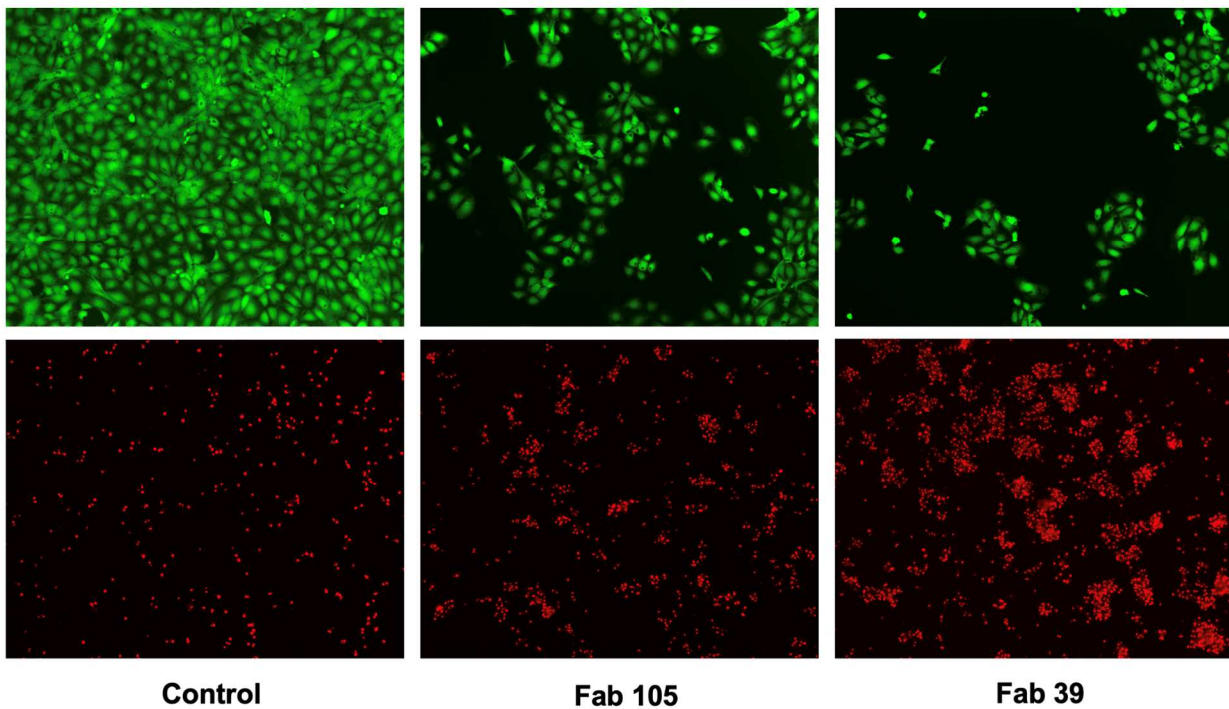


Figure 3-11. Human Fabs cause endothelial cell death *in vitro*

Immortalized transgenic endothelial cells that express human PLXDC1 show significantly greater cell death compared to control Fab at 24-hours. The red signal (propidium iodide) indicates cell death while the green (fluorescein diacetate) signal reflects alive cells.

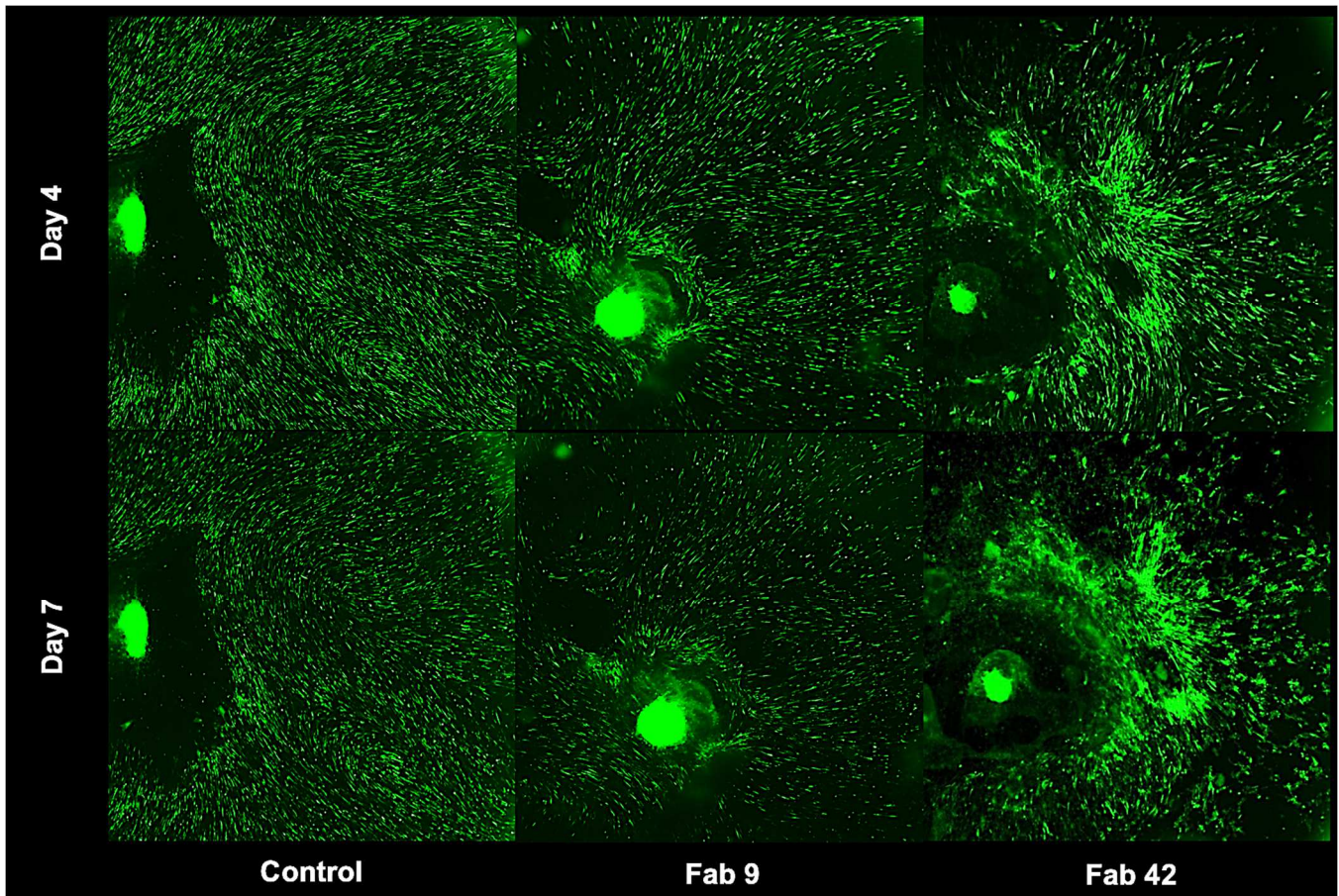


Figure 3-12. Human Fabs cause endothelial cell death in *ex vivo* 3D endothelial cell culture

Ectopically expressed human PLXDC1 in *ex vivo* 3D endothelial cell culture demonstrates killing of endothelial cells by two human Fabs compared to control Fab.

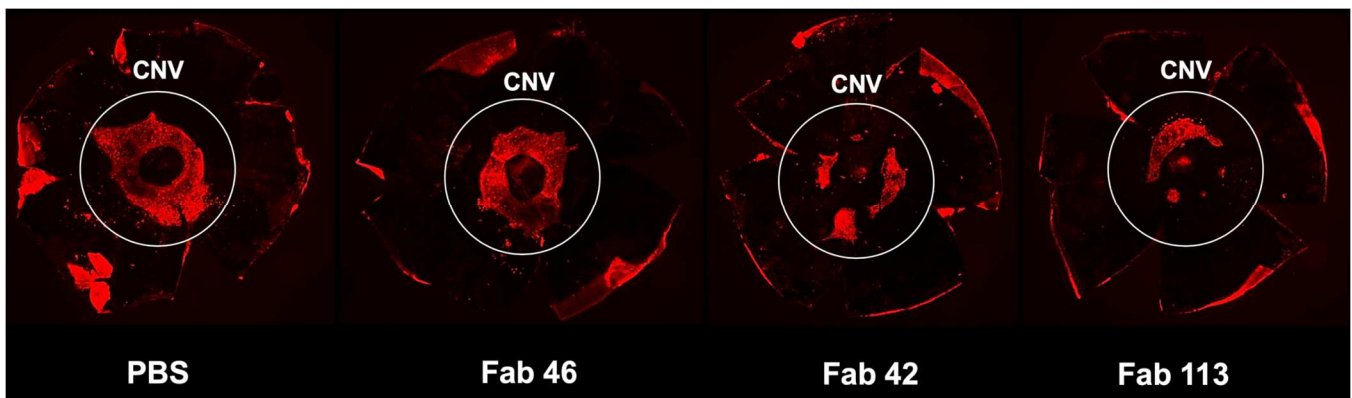


Figure 3-13. Human Fabs cause inhibition of *in vivo* laser-induced choroidal neovascularization

Laser induced choroidal neovascularization treated with various Fabs show partial CNV inhibition compared to control in some but not all human Fabs.

REFERENCES

1. Hunter J. A treatise on the blood, inflammation, and gun-shot wounds. 1794. *Clin Orthop Relat Res.* 2007. doi:10.1097/BLO.0b013e31803dd01c
2. Folkman J. Tumor angiogenesis: therapeutic implications. *N Engl J Med.* 1971. doi:10.1056/NEJM197111182852108
3. Folkman J. Angiogenesis in cancer, vascular, rheumatoid and other disease. *Nat Med.* 1995. doi:10.1038/nm0195-27
4. Carmeliet P, Jain RK. Angiogenesis in cancer and other diseases. *Nature.* 2000. doi:10.1038/35025220
5. Simo R, Carrasco E, Garcia-Ramirez M, Hernandez C. Angiogenic and Antiangiogenic Factors in Proliferative Diabetic Retinopathy. *Curr Diabetes Rev.* 2006. doi:10.2174/157339906775473671
6. Ng EWM, Adamis AP. Targeting angiogenesis, the underlying disorder in neovascular age-related macular degeneration. *Can J Ophthalmol.* 2005. doi:10.1016/S0008-4182(05)80078-X
7. Konisti S, Kiriakidis S, Paleolog EM. Angiogenesis in rheumatoid arthritis. In: *Angiogenesis and Vascularisation: Cellular and Molecular Mechanisms in Health and Diseases.* ; 2013. doi:10.1007/978-3-7091-1428-5_16
8. Heidenreich R, Röcken M, Ghoreschi K. Angiogenesis drives psoriasis pathogenesis. *Int J Exp Pathol.* 2009. doi:10.1111/j.1365-2613.2009.00669.x
9. Ferrara N, Hillan KJ, Gerber H-PP, Novotny W. Discovery and development of bevacizumab, an anti-VEGF antibody for treating cancer. *Nat Rev Drug Discov.* 2004;3(5):391-400. doi:10.1038/nrd1381

10. Kim LA, D'Amore PA. A brief history of anti-VEGF for the treatment of ocular angiogenesis. *Am J Pathol*. 2012. doi:10.1016/j.ajpath.2012.06.006
11. Krebs I, Glittenberg C, Ansari-Shahrezaei S, Hagen S, Steiner I, Binder S. Non-responders to treatment with antagonists of vascular endothelial growth factor in age-related macular degeneration. *Br J Ophthalmol*. 2013. doi:10.1136/bjophthalmol-2013-303513
12. Lux A, Llacer H, Heussen FMA, Jousseaume AM. Non-responders to bevacizumab (Avastin) therapy of choroidal neovascular lesions. *Br J Ophthalmol*. 2007. doi:10.1136/bjo.2006.113902
13. Kurihara T, Westenskow PD, Bravo S, Aguilar E, Friedlander M. Targeted deletion of Vegfa in adult mice induces vision loss. *J Clin Invest*. 2012;122(11):4213-4217. doi:10.1172/JCI65157
14. Quaggin SE. Turning a blind eye to anti-VEGF toxicities. *J Clin Invest*. 2012. doi:10.1172/JCI65509
15. Bauman CR, Spaide RF, Vajzovic L, et al. Retinal vasculitis and intraocular inflammation after intravitreal injection of brodalumab. *Ophthalmology*. April 2020. doi:10.1016/j.ophtha.2020.04.017
16. Manousaridis K, Talks J. Macular ischaemia: A contraindication for anti-VEGF treatment in retinal vascular disease? *Br J Ophthalmol*. 2012. doi:10.1136/bjophthalmol-2011-301087
17. Warren RS, Yuan H, Matli MR, Gillett NA, Ferrara N. Regulation by vascular endothelial growth factor of human colon cancer tumorigenesis in a mouse model of experimental liver metastasis. *J Clin Invest*. 1995. doi:10.1172/JCI117857

18. Kolata G. HOPE IN THE LAB: A special report; A cautious awe greets drugs that eradicate tumors in mice. *New York Times*. 1998.
19. Meadows KL, Hurwitz HI. Anti-VEGF therapies in the clinic. *Cold Spring Harb Perspect Biol*. 2012.
20. Rxlist. Avastin. <https://www.rxlist.com/avastin-drug.htm#indications>.
21. Kreisl TN, Kim L, Moore K, et al. Phase II trial of single-agent bevacizumab followed by bevacizumab plus irinotecan at tumor progression in recurrent glioblastoma. *J Clin Oncol*. 2009. doi:10.1200/JCO.2008.16.3055
22. Friedman HS, Prados MD, Wen PY, et al. Bevacizumab alone and in combination with irinotecan in recurrent glioblastoma. *J Clin Oncol*. 2009. doi:10.1200/JCO.2008.19.8721
23. Minkevich NI, Lipkin VM, Kostanyan IA. PEDF - A Noninhibitory Serpin with Neurotrophic Activity. *Acta Naturae*. 2010;2(3):62-81. doi:10.32607/20758251-2010-2-3-62-81
24. Tombran-Tink J, Johnson L V. Neuronal differentiation of retinoblastoma cells induced by medium conditioned by human RPE cells. *Investig Ophthalmol Vis Sci*. 1989.
25. Tombran-Tink J, Chader GG, Johnson L V. PEDF: A pigment epithelium-derived factor with potent neuronal differentiative activity. *Exp Eye Res*. 1991;53(3):411-414. doi:10.1016/0014-4835(91)90248-D
26. Tombran-Tink J, Barnstable CJ. PEDF: A multifaceted neurotrophic factor. *Nat Rev Neurosci*. 2003. doi:10.1038/nrn1176
27. Dawson DW. Pigment Epithelium-Derived Factor: A Potent Inhibitor of Angiogenesis. *Science (80-)*. 1999;285(5425):245-248. doi:10.1126/science.285.5425.245
28. Crawford SE, Stellmach V, Ranalli M, et al. Pigment epithelium-derived factor (PEDF) in

- neuroblastoma: A multifunctional mediator of Schwann cell antitumor activity. *J Cell Sci.* 2001.
29. Kanda S, Mochizuki Y, Nakamura T, Miyata Y, Matsuyama T, Kanetake H. Pigment epithelium-derived factor inhibits fibroblast-growth-factor-2-induced capillary morphogenesis of endothelial cells through Fyn. *J Cell Sci.* 2005. doi:10.1242/jcs.01686
 30. Cai J, Parr C, Watkins G, Jiang WG, Boulton M. Decreased pigment epithelium-derived factor expression in human breast cancer progression. *Clin Cancer Res.* 2006. doi:10.1158/1078-0432.CCR-06-0094
 31. Doll JA, Stellmach VM, Bouck NP, et al. Pigment epithelium-derived factor regulates the vasculature and mass of the prostate and pancreas. *Nat Med.* 2003. doi:10.1038/nm870
 32. Ek ETH, Dass CR, Choong PFM. Pigment epithelium-derived factor: A multimodal tumor inhibitor. *Mol Cancer Ther.* 2006. doi:10.1158/1535-7163.MCT-06-0107
 33. Becerra SP, Notario V. The effects of PEDF on cancer biology: Mechanisms of action and therapeutic potential. *Nat Rev Cancer.* 2013. doi:10.1038/nrc3484
 34. St. Croix B, Rago C, Velculescu V, et al. Genes expressed in human tumor endothelium. *Science (80-).* 2000. doi:10.1126/science.289.5482.1197
 35. Carson-Walter EB, Watkins DN, Nanda A, Vogelstein B, Kinzler KW, St. Croix B. Cell surface tumor endothelial markers are conserved in mice and humans. *Cancer Res.* 2001.
 36. Pietrzyk Ł, Wdowiak P. Serum TEM5 and TEM7 concentrations correlate with clinicopathologic features and poor prognosis of colorectal cancer patients. *Adv Med Sci.* 2019. doi:10.1016/j.advms.2019.07.001
 37. Czekierdowski A, Stachowicz N, Czekierdowska S, Łoziński T, Gurynowicz G, Kluz T. Prognostic significance of TEM7 and nestin expression in women with advanced high

- grade serous ovarian cancer. *Ginekol Pol.* 2018. doi:10.5603/GP.a2018.0023
38. Carpenter RL, Paw I, Zhu H, et al. The gain-of-function GLI1 transcription factor TGLI1 enhances expression of VEGF-C and TEM7 to promote glioblastoma angiogenesis. *Oncotarget.* 2015. doi:10.18632/oncotarget.4248
39. Zhang Z-Z, Hua R, Zhang J-F, et al. TEM7 (PLXDC1), a key prognostic predictor for resectable gastric cancer, promotes cancer cell migration and invasion. *Am J Cancer Res.* 2015.
40. Meehan B, Appu S, St Croix B, Rak-Poznanska K, Klotz L, Rak J. Age-related properties of the tumour vasculature in renal cell carcinoma. *BJU Int.* 2011. doi:10.1111/j.1464-410X.2010.09569.x
41. Yamaji Y, Yoshida S, Ishikawa K, et al. TEM7 (PLXDC1) in neovascular endothelial cells of fibrovascular membranes from patients with proliferative diabetic retinopathy. *Investig Ophthalmol Vis Sci.* 2008. doi:10.1167/iovs.07-1249
42. Cheng G, Zhong M, Kawaguchi R, et al. Identification of PLXDC1 and PLXDC2 as the transmembrane receptors for the multifunctional factor PEDF. *Elife.* 2014. doi:10.7554/eLife.05401
43. Bagley RG, Rouleau C, Weber W, et al. Tumor endothelial marker 7 (TEM-7): A novel target for antiangiogenic therapy. *Microvasc Res.* 2011;82(3):253-262. doi:10.1016/j.mvr.2011.09.004
44. Shalem O, Sanjana NE, Hartenian E, et al. Genome-Scale CRISPR-Cas9 Knockout Screening in Human Cells. *Science (80-).* 2014;343(6166):84-87. doi:10.1126/science.1247005
45. Joung J, Konermann S, Gootenberg JS, et al. Genome-scale CRISPR-Cas9 knockout and

- transcriptional activation screening. *Nat Protoc.* 2017. doi:10.1038/nprot.2017.016
46. Paoli P, Giannoni E, Chiarugi P. Anoikis molecular pathways and its role in cancer progression. *Biochim Biophys Acta - Mol Cell Res.* 2013. doi:10.1016/j.bbamcr.2013.06.026
47. Illing M, Molday LL, Molday RS. The 220-kDa rim protein of retinal rod outer segments is a member of the ABC transporter superfamily. *J Biol Chem.* 1997. doi:10.1074/jbc.272.15.10303
48. Joung J, Konermann S, Gootenberg JS, et al. Genome-scale CRISPR-Cas9 knockout and transcriptional activation screening. *Nat Protoc.* 2017. doi:10.1038/nprot.2017.016
49. Kimelman D, Xu W. β -Catenin destruction complex: Insights and questions from a structural perspective. *Oncogene.* 2006. doi:10.1038/sj.onc.1210055
50. Mas-Moruno C, Rechenmacher F, Kessler H. Cilengitide: The First Anti-Angiogenic Small Molecule Drug Candidate. Design, Synthesis and Clinical Evaluation. *Anticancer Agents Med Chem.* 2011. doi:10.2174/187152010794728639
51. Yamada S, Bu XY, Khankaldyyan V, Gonzales-Gomez I, McComb JG, Laug WE. Effect of the angiogenesis inhibitor Cilengitide (EMD 121974) on glioblastoma growth in nude mice. *Neurosurgery.* 2006. doi:10.1227/01.NEU.0000245622.70344.BE
52. Reardon DA, Fink KL, Mikkelsen T, et al. Randomized phase II study of cilengitide, an integrin-targeting arginine-glycine-aspartic acid peptide, in recurrent glioblastoma multiforme. *J Clin Oncol.* 2008. doi:10.1200/JCO.2008.16.7510
53. Stupp R, Hegi ME, Gorlia T, et al. Cilengitide combined with standard treatment for patients with newly diagnosed glioblastoma with methylated MGMT promoter (CENTRIC EORTC 26071-22072 study): a multicentre, randomised, open-label, phase 3

- trial. *Lancet Oncol.* 2014;15(10):1100-1108. doi:10.1016/S1470-2045(14)70379-1
54. Tucci M, Stucci S, Silvestris F. Does cilengitide deserve another chance? *Lancet Oncol.* 2014. doi:10.1016/S1470-2045(14)70462-0
55. Krishan Maggon. Monoclonal Antibody “Gold Rush.” *Curr Med Chem.* 2007;14(18):1978-1987. doi:10.2174/092986707781368504
56. Liu JKH. The history of monoclonal antibody development - Progress, remaining challenges and future innovations. *Ann Med Surg.* 2014. doi:10.1016/j.amsu.2014.09.001
57. Singh S, Kumar NK, Dwiwedi P, et al. Monoclonal Antibodies: A Review. *Curr Clin Pharmacol.* 2018;13(2):85-99. doi:10.2174/1574884712666170809124728
58. KÖHLER G, MILSTEIN C. Continuous cultures of fused cells secreting antibody of predefined specificity. *Nature.* 1975;256(5517):495-497. doi:10.1038/256495a0
59. Tomita M, Tsumoto K. Hybridoma technologies for antibody production. *Immunotherapy.* 2011. doi:10.2217/imt.11.4
60. Smith GP. Phage Display: Simple Evolution in a Petri Dish (Nobel Lecture). *Angew Chemie - Int Ed.* 2019. doi:10.1002/anie.201908308
61. Boder ET, Raeeszadeh-Sarmazdeh M, Price JV. Engineering antibodies by yeast display. *Arch Biochem Biophys.* 2012;526(2):99-106. doi:10.1016/j.abb.2012.03.009
62. Lambert V, Lecomte J, Hansen S, et al. Laser-induced choroidal neovascularization model to study age-related macular degeneration in mice. *Nat Protoc.* 2013. doi:10.1038/nprot.2013.135
63. Lonberg N. Human antibodies from transgenic animals. *Nat Biotechnol.* 2005. doi:10.1038/nbt1135
64. Williams DG, Matthews DJ, Jones T. Humanising Antibodies by CDR Grafting. In:

- Antibody Engineering*. Berlin, Heidelberg: Springer Berlin Heidelberg; 2010:319-339.
doi:10.1007/978-3-642-01144-3_21
65. Mayes PA, Hance KW, Hoos A. The promise and challenges of immune agonist antibody development in cancer. *Nat Rev Drug Discov*. 2018. doi:10.1038/nrd.2018.75
 66. Suomivuori CM, Latorraca NR, Wingler LM, et al. Molecular mechanism of biased signaling in a prototypical G protein-coupled receptor. *Science (80-)*. 2020.
doi:10.1126/science.aaz0326
 67. Wingler LM, Skiba MA, McMahon C, et al. Angiotensin and biased analogs induce structurally distinct active conformations within a GPCR. *Science (80-)*. 2020.
doi:10.1126/science.aay9813
 68. Chazenbalk GD, Pichurin P, Chen CR, et al. Thyroid-stimulating autoantibodies in Graves disease preferentially recognize the free A subunit, not the thyrotropin holoreceptor. *J Clin Invest*. 2002. doi:10.1172/JCI0215745
 69. Rapoport B, Chazenbalk GD, Jaume JC, McLachlan SM. The Thyrotropin (TSH)-Releasing Hormone Receptor: Interaction with TSH and Autoantibodies 1. *Endocr Rev*. 1998;19(6):673-716. doi:10.1210/edrv.19.6.0352
 70. Kaithamana S, Fan J, Osuga Y, Liang SG, Prabhakar BS. Induction of experimental autoimmune Graves' disease in BALB/c mice. *J Immunol*. 1999;163(9):5157-5164.
 71. Costagliola S, Rodien P, Many MC, Ludgate M, Vassart G. Genetic immunization against the human thyrotropin receptor causes thyroiditis and allows production of monoclonal antibodies recognizing the native receptor. *J Immunol*. 1998.
 72. Nagayama Y, Kita-Furuyama M, Ando T, et al. A Novel Murine Model of Graves' Hyperthyroidism with Intramuscular Injection of Adenovirus Expressing the Thyrotropin

Receptor. *J Immunol.* 2002;168(6):2789-2794. doi:10.4049/jimmunol.168.6.2789